BAERLIN2014 – stationary measurements and source apportionment at an urban background station in Berlin, Germany

Erika von Schneidemesser[1], Boris Bonn[1*], Tim M. Butler[1], Christian Ehlers[2α], Holger Gerwig[3], Hannele Hakola[4], Heidi Hellén[4], Andreas Kerschbaumer[5], Dieter Klemp[2], Claudia Kofahl[2β], Jürgen Kura[3], Anja Lüdecke[3], Rainer Nothard[5], Axel Pietsch[3], Jörn Quedenau[1], Klaus Schäfer[6], James J. Schauer[7], Ashish Singh[1], Ana-Maria Villalobos[7], Matthias Wiegner[8], Mark G. Lawrence[1]

[1]Institute for Advanced Sustainability Studies (IASS), D-14467 Potsdam, Germany
[2]IEK-8, Research Centre Jülich, D-52425 Jülich, Germany
[3]Division Environmental Health and Protection of Ecosystems, German Environment Agency, D-06844 Dessau-Roßlau, Germany
[4]Finnish Meteorological Institute, FI-00560 Helsinki, Finland
[5]Senate Department for the Environment, Transport and Climate Protection, D-10179 Berlin, Germany
[6]Institute of Meteorology and Climate Research, Atmospheric Environmental Research (IMK-IFU), Karlsruhe Institute of Technology (KIT), D-82467 Garmisch-Partenkirchen, Germany
[7]Environmental Chemistry and Technology Program, University of Wisconsin-Madison, Madison 53705, WI, USA
[8]Ludwig-Maximilians-Universität, Meteorological Institute, D-80333 Munich, Germany
*now at: Chair of Ecosystem Physiology, Institute of Forest Sciences, Albert-Ludwig Universität, D-79110 Freiburg, Germany
αnow at: Fachbereich 42: Kontinuierliches Luftqualitätsmessnetz, Landesamt für Natur, Umwelt und Verbraucherschutz NRW, D-45133 Essen, Germany
βnow at: Institut für Physikalische Chemie, Georg-August-Universität, D-37077 Göttingen, Germany

Correspondence to Erika von Schneidemesser (evs@iass-potsdam.de)

Abstract. The Berlin Air quality and Ecosystem Research: Local and long-range Impact of anthropogenic and Natural hydrocarbons (BAERLIN2014) campaign was conducted during the three summer months (June-August) of 2014. During this measurement campaign, both stationary and mobile measurements were undertaken to address complementary aims. This paper provides an overview of the stationary measurements and results that were focused on characterization of gaseous and particulate pollution, including source attribution, in the Berlin-Potsdam area, and quantification of the role of natural sources in determining levels of ozone and related gaseous pollutants. Results show that biogenic contributions to ozone and particulate matter are substantial. One indicator for ozone formation, the OH reactivity, showed a 31% (0.82 ± 0.44 s^{-1}) and 75% (3.7 ± 0.90 s^{-1}) contribution from biogenic NMVOCs for urban background (2.6 ± 0.68 s^{-1}) and urban park (4.9 ± 1.0 s^{-1}) location, respectively, emphasizing the importance of such locations as sources of biogenic NMVOCs in urban areas. A comparison to NMVOC measurements made in Berlin ca. 20 years earlier generally show lower levels today for anthropogenic NMVOCs. A substantial contribution of secondary organic and inorganic aerosol to PM$_{10}$ concentrations was quantified. In addition to secondary aerosols, source apportionment analysis of the organic carbon fraction identified the contribution of biogenic (plant-based) particulate matter, as well as primary contributions from vehicles, with a larger contribution from diesel compared to gasoline vehicles, as well as a relatively small contribution from wood burning, linked to measured levoglucosan.

46

1 Introduction

47

48

49 Air pollution and climate change are two of the most prescient environmental problems of our age. Recent

50 research from the Global Burden of Disease study and others attribute over 3 million premature deaths to

51 outdoor air pollution globally in 2013 (Brauer et al., 2016;Lelieveld et al., 2015;WHO, 2016). A report by the

52 World Bank (WorldBank, 2016) estimated the 2013 welfare losses owing to ambient surface level $PM_{2.5}$ and O_3

53 air pollution to be equivalent to 5% of GDP in Europe, and often more in other world regions. Studies have

54 shown that a changing climate will exacerbate ozone owing to increased temperatures and other factors, such as

55 additional meteorological parameters and less effective emissions controls, that are favorable to ozone formation

56 (Jacob and Winner, 2009;Rasmussen et al., 2013). One such factor is a projected increase in biogenic volatile

57 organic compound emissions, such as isoprene or monoterpenes. While these increases are expected to be

58 compensated for by much larger declines in anthropogenic emissions, as also indicated in other studies e.g.

59 Colette et al. (2013) or West et al. (2013), there are additional impacts that are not yet captured by the models,

60 such as those of secondary organic aerosol (SOA) among others, that show that such estimates of climate change

61 effects are likely underestimated (Geels et al., 2015). While significant reductions in O_3 precursor emissions

62 have been observed over the past couple decades, and peak ozone levels have been declining over much of

63 north-western Europe, a comparable reduction in mean ozone has not followed (Derwent, 2008;Ehlers et al.,

64 2016). This is particularly relevant for countries where the majority of the population resides in cities. In Europe

65 during 2012-2014, more than 85% of the urban population has been exposed to air pollutant concentrations of

66 ozone and $PM_{2.5}$ exceeding the recommended WHO limit values for the protection of human health, as well as

67 substantial exceedances at the roadside of nitrogen dioxide (NO_2) (EEA, 2016). In this context, it is crucial that

68 we further improve our understanding of the sources of air pollutants in urban areas, as well as the contribution

69 of natural sources to secondary pollutants such as ozone. This will allow for approaches that can better target the

70 most relevant sources for mitigation, as well as accounting for the linkages between air quality and climate

71 change in developing strategies for action on climate change and the reduction of air pollution, to improve health

72 and create more livable cities.

73 The Berlin Air quality and Ecosystem Research: Local and long-range Impact of anthropogenic and

74 Natural hydrocarbons 2014 (BAERLIN2014) campaign aimed to address some of these issues in the context of

75 the Berlin-Potsdam urban area. The campaign had three main aims, (1) characterization of gaseous and

76 particulate pollution, including source attribution, in the Berlin-Potsdam area, (2) quantification of the role of

77 natural sources, specifically vegetation, in determining levels of gaseous pollutants, specifically ozone, and (3)

78 improved understanding of the heterogeneity of pollutants throughout the city. In this paper, only aims (1) and

79 (2) will be addressed. An overview paper describing the mobile measurements, which focused more on aim (3)

80 was published previously (see Bonn et al. (2016)). Because of the focus on ozone and secondary pollutant

81 formation, the campaign was conducted during the three summer months (June-August) of 2014, i.e. the time of

82 maximum ozone pollution levels. Furthermore, while the mobile measurements covered the larger Berlin-

83 Potsdam area, the stationary measurements were focused on an urban background location within the center of

84 Berlin.

85 The unique characteristics of Berlin were particularly relevant to this study, in that it is a large urban

86 area (population ca. 3.5 million) with significant vegetation. Of the ca. 890 km^2 that Berlin covers, ca. 34% of

87   the land surface area is covered by vegetated areas and 6% by water (Senatsverwaltung für Stadtentwicklung III

88   F, 2010). An existing air quality monitoring network (in German: Berliner Luftgüte Messnetz, abbreviated

89   BLUME) provided data on which the campaign could build and leverage. Data from the 16 stations that

90   comprised the BLUME network showed that the EU 8-hour ozone target value of 120 µg m^{-3} was exceeded 12-

91   13 times at each of the two urban background stations that measure ozone (MC010 & MC042) and between 12-

92   21 times per station at the stations on the periphery of the city (referred to here as Berlin rural stations) in 2014

93   (Stülpnagel et al., 2015). Six of these exceedances in the urban background occurred during the BAERLIN2014

94   campaign. Furthermore, the regulatory limit value for annual NO$_2$ of 40 µg m^{-3} was exceeded at all six roadside

95   stations in 2014, and although the annual PM$_{10}$ limit value was met, four out of five traffic stations where PM$_{10}$

96   was measured also exceeded the daily limit value of 50 µg m^{-3} more than the allowed 35 times; the exceedances

97   at the urban background and Berlin rural stations ranged from 14 to 34 times (Stülpnagel et al., 2015). In short,

98   the issue of air pollution has been recognized in Berlin as being in need of action. In this paper, we focus on the

99   stationary measurements conducted at the urban background site in the Berlin city center. A brief overview is

100 given of the suite of measurements conducted and the results obtained. This is followed by more detailed

101 analysis of (1) the NMVOC data and the role in ozone formation including a comparison to a previous study in

102 London and Paris (von Schneidemesser et al., 2011), as well as other urban areas, and (2) source apportionment

103 analysis of PM$_{10}$ filter samples, including a rough comparison of the results to existing emission inventories.

104

105 **2   Methods**

106

107 A complete list of the parameters measured and their associated instrument descriptions are summarized in Table

108 1.

109

110 **2.1 Site description**

111   The monitoring station that was the basis for the stationary measurements during the BAERLIN2014

112 campaign was AirBase station DEBE034, which is maintained as part of the Berlin air quality measurement

113 network (BLUME; BLUME network code MC042), and was located at the corner of Nansenstrasse and

114 Framstrasse in the Neukölln district, in southeast central Berlin (52° 29' 21,98" N, 13° 25' 51,08" E) in a

115 predominantly residential neighborhood, as shown in Figure 1. The station was located on the street corner next

116 to a kindergarten and was classified as an urban background station. According to the location placement

117 dictated by the EU Directive definition (EC, 2008), locations that are situated away from any strong point

118 sources including major roads, typically in a residential neighborhood, but still in the urban core influenced by

119 all sources upwind of the station are classified as urban background. These sites should in theory be

120 representative of the general levels of pollution observed in a city and are used to assess exposure of the general

121 population to air pollutants. This station will likely experience a comparatively high fraction of traffic-related

122 emissions, since some fairly large inner-city thoroughfares were located within a 1 km radius of the site, but as

123 appropriate for an urban background station will not be dominated by traffic like a site located at a major

124 intersection. In addition, a measurement van was used to augment the capacity of the measurement station and

125 was located approximately 5 meters from the station, parked at the curb of the street (see Figure 1). Finally,

126 owing to the presence of taller trees in that part of city, including in the vicinity of the monitoring station, one

127 instrument (ceilometer) was located on the roof of the kindergarten to achieve an unobstructed view skywards,
128 approximately 5 meters on the opposite side of the measurement station to the van.

129   A number of NMVOC canister samples were taken in locations throughout the city as part of the mobile
130 measurements that augmented the stationary measurements in Neukölln. A subset of these were included in the
131 companion paper to this one covering the mobile measurements (Bonn et al., 2016). These sites where multiple
132 NMVOC canister samples were taken include Altlandsberg, Plänterwald, the Tiergarten Tunnel, and the AVUS
133 Motorway during a traffic jam. Further details to the sampling environment can be found in Table 2. For more
134 information on locations and/or sampling, see also Bonn et al. (2016).

135

2.2 Instrument descriptions

137   Complementing the BLUME measurements (see Stülpnagel et al., (2015) or Geiß et al., (2017) for
138 details) were additional PM_{10} filter samples collected for elemental carbon (EC) and organic carbon (OC), ions,
139 and organic tracer analysis; intermittent canister and cartridge samples for the quantification of non-methane
140 volatile organic compounds (NMVOCs) from an inlet next to the PM_{10} inlet on the roof of the measurement
141 station; a quadrupole Proton Transfer Reaction Mass Spectrometre (high sensitivity PTR-MS, Ionicon) up in the
142 van for the measurement of NMVOCs; a set of particle instruments to measure number concentration, size
143 distribution and surface area also located in the van (section 2.2.4); and a ceilometer CL51 (Vaisala GmbH,
144 Hamburg) situated on the roof of the kindergarten. A complete list of instruments, parameters measured, and
145 references for the methods used are provided in Table 1. Further details for the NMVOC measurements are
146 provided in Table S1. Additional information is provided below.

147

2.2.1   NMVOC Canister Samples

149   The canisters were prepared to remove ozone using a heated silco-steel capillary (120 °C) prior to
150 sampling. The cylinders were then pressurized using synthetic air to reduce the relative humidity of the sample.
151 All NMVOC canister samples taken at Neukölln had a 20 minute sampling duration. After sampling, the
152 canisters were promptly shipped to FZJ for analysis by GC-FID-MS and were analyzed with no more than five
153 days between sampling and analysis. Analysis was done using a gas chromatographic system based on a
154 conventional gas chromatograph (Agilent 6890) equipped with a flame ionization detector (FID), and a mass
155 spectrometer (Agilent 5975C MSD) for the identification of the trace species. To analyze VOCs at trace gas
156 levels, a cryogenic pre-concentration was used, consisting of a sample loop (silco steel, 20 cm length, inner
157 diameter 2 mm) which was cooled down with cold gas above liquid nitrogen (see also Figure 14 in Ehlers et al.,
158 (2016)). A volume of 800 mL was pre-concentrated in the sample loop at a flow of 80 mL min^{-1}.

159   Subsequently, the sample was thermally desorbed at 120° C and injected on a capillary column (DB-1,
160 120 m, 0.32 mm ID, 3µm film thickness). After injection, the column was kept isothermal at -60°C for 5 min,
161 then heated to 200° C at a rate of 4° min^{-1} and finally maintained at 220° C for 10 min. Signals were gathered
162 from a flame ionization detector and a MSD, which each received 50% of the column output through a split
163 valve. Analysis of one sample lasted for about 90 min, and sets of 10 cylinders (stainless steel canister, volume:
164 6 L, Supelco Co., Bellefonte, PA, USA) could be analyzed by unattended operation.

165   The impact of canister transport and storage was assessed: C_2 - C_{11} alkanes, alkenes and aromatic
166 compounds were found to be stable within 5% over three days compared with an instantaneously analysed
167 sample. Oxygenated compounds differed by up to 10% over the same time period. In addition, measurement

168 accuracy depends on the uncertainty of the calibration standard (< 5% between true and declared gas

169 concentrations, (Apel-Riemer Environmental Inc.) and that of the mass-flow controller (< 2% deviation, MKS

170 Instruments, Wilmington, MA, USA). Integration uncertainties ($\Delta\mu VOC$) of the peak areas were dependent on

171 their respective detection limits (DL_i), which are estimated as in equation 1.

172
$$\Delta\mu VOCi \approx \begin{cases} DL_i & \text{for } \mu VOC_i \text{ nextto } DL_i \\ (0,03-0,06)*\mu VOC_i & \text{otherwise} \end{cases} \quad (1)$$

173 Apart from concentrations and their respective detection limits geometrical addition of all these factors yielded

174 overall experimental uncertainties of less than 10% (for a detailed discussion refer to Urban (2010)).

175

176 **2.2.1.1 Canister Samples and OH Reactivity Calculations**

177 While a total of 103 compounds were quantified by GC-MS in the canister samples, not all of those

178 compounds were regularly detected in the samples. Furthermore, to be able to make reasonable comparisons

179 with previous work regarding the contribution of different compound classes to the measured mixing ratios of

180 NMVOCs, as well as the OH reactivity attributed to these NMVOCs, a subset of the compounds was selected

181 and used in the analysis. This subset was based on a number of papers in the literature that were also done in

182 urban areas, and those compounds that were regularly included in OH reactivity calculations (e.g. (Dolgorouky

183 et al., 2012;Gilman et al., 2009;Goldan et al., 2004;Liu et al., 2008)). This includes 57 NMVOCs (see SI).

184 Furthermore, even if all compounds were included, there would still be missing reactivity that is not captured

185 and because no OH measurements were made, the amount of missing reactivity cannot be reliably quantified.

186 Owing to an undetermined source of contamination at the urban background site, the measurement of n-butane

187 was compromised, and was therefore not included among the NMVOCs despite typically being reported in the

188 literature. The data subsequently presented in this paper from the canister samples includes only these 57

189 compounds unless otherwise noted. For a complete list of the 103 compounds measured in the samples,

190 including the concentrations reported for a subset of the samples discussed here, please see Bonn et al. (2016).

191 A number of canister samples were taken at different locations throughout the city, some with multiple

192 measurements and some single samples. Five locations had multiple samples, including the main measurement

193 site at the urban background station (DEBE034) in Neukölln (n=18), Plänterwald (n=11), Altlandsberg (n=10),

194 the Tiergarten Tunnel (n=9), and the AVUS motorway during a traffic jam (n=2). All samples were taken during

195 the month of August, will all samples except those in Neukölln taken on one day for any given location (Bonn et

196 al., 2016). The samples in the Tiergarten tunnel and on the motorway are most indicative of NMVOC emissions

197 from traffic.

198

199 **2.2.2 NMVOC Cartridge Samples**

200 NMVOCs (aromatic hydrocabons, terpenes, C_6-C_{10} alkanes) were collected into stainless steel

201 cartridges (6.3 mm ED x 90 mm, 5.5 mm ID) filled with Tenax-TA (60/80 mesh, Supelco, Bellafonte, USA) and

202 Carboback-B (60/80 mesh, Supelco, Bellafonte, USA) by using a flow rate of 100 ml min^{-1} with a sampling time

203 of 1 - 4.5 h (Mäki et al., 2017). To prevent the degradation of BVOC by O_3, a catalyst heated to 150ºC was used.

204 Individual VOCs were identified and quantified using a thermal desorption instrument (Perkin-Elmer

205 TurboMatrixTM 650, Waltham, USA) connected to a gas chromatograph (Perkin-Elmer® Clarus® 600,

206 Waltham, USA) with a DB-5MS (60 m, 0.25 mm, 1 µm) column and a mass selective detector (Perkin-Elmer®

207 Clarus® 600T, Waltham, USA). Five-point calibration was utilised using liquid standards in methanol solutions.

208 Standard solutions were injected onto adsorbent tubes that were flushed with nitrogen (HiQ N_2 6.0 >99.9999%,

209 Linde AG, Pullach, Germany) flow (100 ml min^{-1}) for 10 min in order to remove methanol. For aromatic

210 hydrocarbons (benzene, toluene, ethylbenzene, p/m-xylene, styrene, o-xylene, propylbenzene, ethyltoluenes,

211 trimethylbenzenes) detection limits (LODs) varied between 5 and 60 ng m^{-3}, for $C_{6\text{-}10}$ alkanes (hexane, heptane,

212 octane, nonane, decane) between 5 and 10 ng m^{-3} and for isoprene LOD was 21 ng m^{-3}. The quantified

213 monoterpenes (MT) were α-pinene, camphene, β-pinene, Δ^3-carene, p-cymene, limonene, 1,8-cineol, nopinone,

214 terpinolene and bornylacetate with limit of detection in the range of 3-17 ng m^{-3}; sesquiterpenes were

215 longicyclene, iso-longifolene, aromadendrene, β-caryophyllene and α-humulene with LOD of 20 ng m^{-3}.

216

217 2.2.3 NMVOC PTR-MS Measurements

218 In addition to canister and cartridge samples, NMVOCs were continuously measured over time by a high-

219 sensitivity proton transfer reaction mass spectrometer (PTR-MS, Ionicon, built in 2008) (Lindinger et al., 1993).

220 In brief NMVOCs with a higher proton affinity than water vapor were charged via H_3O^+ ions and subsequently

221 mass selectively detected by applying a distinct electric field strength for the individual masses selected. More

222 details on the techniques can be found elsewhere (Blake et al., 2009). In total, 72 selected NMVOCs were

223 measured between June 11 and August 29, 2014 via a heated inlet (T = 60°C) at street level out of the street

224 facing window of a measurement van (MW088) at approximately 2.5 m above surface. Note that this PTR-MS

225 detected integer ion mass numbers only and no time of flight option was available for this version. Selection of

226 masses were based on two aspects: first, typical mass to charge (m/z) ratios for anthropogenic and biogenic

227 sources like benzene, toluene, isoprene and terpenes, and second, on mass scan results conducted once a week

228 throughout the campaign period. In this way some masses changed during the total observation time because of

229 changed scan intensities and the limited number of masses to be selected. Time resolution was set to 270 s, i.e.

230 4.5 min. The dataset was averaged after the campaign for 30 min and 1h for comparison with other less time

231 resolved measurement data. Instrument parameters were set as follows: U_{QL} = 50 V, U_N = 60 V, U_{SO} = 70.3 V

232 and U_S = 113.9 V. The intensity of the reference ion signal for detection efficiency, i.e. m/z = 21, was recorded

233 as $(4.4\pm1.0)\times10^7$ counts per second. For more details on the set-up see Bourtsoukidis et al. (2014). A list of all

234 recorded masses can be found in the supporting online information. Because the PTR-MS technique does not

235 allow for a detailed chemical structure analysis, the cartridge and canister samples were used as complementary

236 information as to the identity of masses with more than a single compound present.

237

238 2.2.4 Particle Number Concentration and Surface Area Measurements

239 The aerosol inlet was located 3.5 m above ground, about 1 m above the measurement van roof, attached

240 to an aerosol splitter (Leibniz Institute for Tropospheric Research (TROPOS), "Kuh"). A LVS pump (Leckel

241 GmbH, Berlin) operated at 1 m³ h^{-1} corresponding to an aerosol flow of 138 cm^3 sec^{-1} and a PM10-head (Leckel

242 GmbH, Berlin) suitable for cut of at 10 µm with 2.3 m³ h^{-1} was used to reduce diffusion losses. This served all

243 particle measurement instruments.

244 The instruments that measured particle number (PN) and particle size distribution included a GRIMM

245 1.108 (particle sizes in optical equivalent diameter, GRIMM Aerosol Technik GmbH & Co. KG, Ainring),

246 GRIMM 5.403, and GRIMM 5.416 (particle sizes in mobility equivalent diameter). Sampling average was

247 mostly 1 min and 8 minutes for Grimm 5.403.

248   The GRIMM 5.416, a condensation particle counter with n-butanol, provided total PN count over a size
249 range from 4-3000 nm at a flow rate of 1.5 L min^{-1}, and the uncertainty for 1 min sampling was ± 0.1% or ± 15
250 cm^{-3} (Helsper et al., 2008;Wiedensohler et al., 2017). The GRIMM 5.403, a scanning mobility particle sizer
251 equipped with a long DMA combined with a CPC with n-butanol measured particle number concentrations with
252 size distribution information for particles between 10-1100 nm at a sample flow rate of 0.3 L min^{-1} and a sheath
253 flow rate of 3 L min^{-1}. For technical details see Heim et al., (2004). The uncertainty associated with the
254 measurement is size dependent, with an uncertainty range of 10-15% in the lowermost size range and ca. 2-3%
255 in the upper size range, and a total of 44 size bins. The GRIMM 1.108, a portable laser aerosol spectrometer and
256 dust monitor measured particle number concentration with size distribution information, covering 350-22500
257 nm, with a sampling flow rate of 1.5 L min^{-1}. Particle number concentrations were determined for 15 size bins
258 with an uncertainty of ± 3%. For technical details see Görner et al. (2012).

259   The TSI Nanoparticle surface area monitor 3550 (NSAM) measured lung deposable surface area for
260 particle sizes ranging from 10-1000 nm at a flow rate of 2.5 L min^{-1}. These values are reported in units of µm^2
261 cm^{-3} corresponding to empirically derived parameters that correspond to the regions where the particles are
262 deposited in the lung. Alveolar deposition was measured. Measurement accuracy for the NSAM was ± 20% for
263 both parameters. Further instrument and measurement details are described elsewhere (Kaminski et al.,
264 2013;VDI, 2017).

265   The NSAM was calibrated at the German Environment Agency (UBA, Langen) with instruments from
266 IUTA, Duisburg (Kaminski, 2011), the GRIMM 1.108 was sent in for maintenance and re-calibrated at the
267 manufacturer prior to use in the campaign, while all other instruments were calibrated a priori at the TROPOS
268 aerosol calibration facility in Leipzig (Weinhold, 2014).

269   A continuous aerosol size distribution (0.01 µm to 30 µm) was created using a combination of GRIMM
270 5.403 (0.01 µm to 1.1 µm) and GRIMM 1.108 (0.3 µm to 30 µm). Averaged 1-h size distribution from both
271 particle instruments were merged to create a full size distribution from 0.01 to 30 µm. Size distributions from the
272 two analyzers were merged by considering GRIMM 5.403 for particles sizes <1.1 µm and sizes equal or above
273 1.1 µm uses GRIMM 1.108. At 1.1 µm both individual logarithmic size bin boundaries of the 5.403, and 1.108
274 were most similar allowing "a smooth merge" without losing any size bins. We also assumed that the particles
275 were spherical and thus no adjustments were made in the size bins, nor were any adjustments made for possible
276 differences in aerodynamic vs optical derivation of diameter.

277

278 **2.2.5   Ceilometer**
279   State-of-the-art ceilometers provide the vertical profile of aerosol backscatter (Wiegner et al., 2014).
280 There are numerous approaches to estimate the mixing layer height (MLH) from the measured profile; the
281 underlying assumption is that at the top of the mixing layer aerosol concentration drastically drops resulting in a
282 pronounced decrease of backscattered signal intensity. Measurements in the framework of BAERLIN2014 were
283 performed with a Vaisala ceilometer CL51 (Münkel, 2007;Geiß et al., 2017). This instrument is eye-safe (class
284 1M), operated fully automated and unattended. The diode laser emits at a wavelength of 910 nm; the absorption
285 by water vapour can be ignored as long as only the MLH is to be determined (Wiegner and Gasteiger, 2015).
286 Laser power and window contamination are permanently monitored to ensure long-term stability. Due to the one
287 lens design the lowest detectable layers are around 50 m, and the system is capable to cover an altitude range

288 greater than 4000 m, topping out around 8 km. Signals are pre-processed, e.g. for the suppression of noise
289 generated artefacts. The range resolution is 10 m, and the temporal averaging is 10 min.

290   The heights of the near surface aerosol layers were analysed by a gradient method from the backscatter
291 profiles in real-time (Emeis et al., 2008) with a MATLAB-based software which is provided by the manufacturer
292 and has been improved continuously (Münkel et al., 2011). The minima of the vertical gradient is used to
293 provide an estimate of the MLH (Emeis et al., 2007). All MLH data presented are following this method (for
294 more detail see Schäfer et al. (2015)) unless otherwise noted. The influence of different options of the
295 proprietary software and an comparison with the more sophisticated approach COBOLT (COntinuous BOundary
296 Layer Tracing) on the retrieved MLH is discussed in detail by Geiß et al. (2017). It was found that the
297 proprietary software slightly tends to overestimate the MLH compared to COBOLT.

298   The various instruments outlined above had differing sampling times and so for those instruments that
299 provided real-time or higher time resolution data, a 30 minute average will be used in the data presented here for
300 comparability.

301

302 **2.2.6 PM_{10} Filter Analysis**

303   Prior to sampling, the quartz fiber filters were baked at 800°C under synthetic air to remove impurities.
304 Post-sampling, the PM_{10} filters were analyzed for total mass, elemental carbon (EC), water soluble and total
305 organic carbon, chloride, sulfate, nitrate, sodium, ammonium, potassium, calcium, and organic tracers.
306 HYSPLIT back trajectories (based on GDAS meteorological data) were calculated for 72 hours over the time
307 period of each filter with a new trajectory each 6 hours for air masses ending at ground level (at the monitoring
308 station) (Stein et al., 2015). Back trajectory plots are included in the Supplemental Information following the
309 final filter groups. Based on similarities in the bulk composition analysis and HYSPLIT back trajectory
310 information, the filters were grouped before being extracted and analyzed for organic tracers. Not all filters were
311 included in these groups, so as to create groups that showed significant similarities. Some individual filters were
312 therefore also excluded from the organic tracer analysis because of a lack of remaining OC mass.

313   PM_{10} mass was first quantified gravimetrically and then analyzed for elemental and organic carbon.
314 For this the filter samples were heated to 750°C in an oxygen stream. The gas stream was then passed through an
315 oxidation catalyst to ensure complete oxidation of the organic carbon to carbon dioxide (CO_2). In contrast to the
316 organic carbon, elemental carbon is directly oxidized at higher temperatures without the requirement of a
317 catalyst. The organic carbon, as CO_2, was then detected using a cavity ring-down spectrometer (Picarro Inc.).
318 The distinction between the elemental and organic carbon fractions in the samples was based on the temperature
319 profile during the analysis. For more details see Ehlers (2013) and Kofahl (2012).

320   A portion of the filter (1.5 cm^2) was water extracted to determine water soluble organic carbon (WSOC)
321 using a TOC-V SCH Shimadzu total organic carbon analyzer (Miyazaki et al., 2011;Yang et al., 2003). The
322 remaining amount of OC was calculated as water insoluble organic carbon (WIOC). A fraction of the remaining
323 solution was used to analyze for water soluble anions and cations by ion chromatography (Dionex ICS 2100 and
324 Dionex ICS 100) (Wang et al., 2005). For the organic tracer analysis, filters were composited as per the bulk
325 composition and HYSPLIT determined groups and extracted with 50/50 dichloromethane and acetone by
326 sonication, an aliquot was derivatized and analyzed by GC-MS (GC-6980, quadrupole MS-5973, Agilent
327 Technology) for organic molecular marker compounds, as described in more detail by Villalobos et al. (2015)
328 and references therein. Approximately 150 organic tracer species were analyzed for, of which less than 100 had

329   concentrations regularly above the detection limit. A limited subset of these was then used in the source
330   apportionment analysis.

331

2.3   Chemical Mass Balance for Source Apportionment

333   A chemical mass balance analysis of the organic carbon fraction of the PM_{10} filter samples was carried
334   out using the organic tracer information. Source apportionment analysis using the CMB technique provides an
335   effective variance least squares solution for a set of linear equations that include the uncertainties of the input
336   measurements, and have been applied to the mass balance receptor model (Watson et al., 1984). As such, it
337   allows for the estimation of the contribution of different source categories to the ambient concentrations
338   measured at any one location, in this case an urban background site in Berlin. The species included in the CMB
339   analysis were levoglucosan, 17α(H)-21β(H)-30-norhopane, 17α(H)-21β(H)-hopane, benzo(b)fluoranthene,
340   benzo(k)fluoranthene, benzo(e)pyrene, benzo(a)pyrene, and C27-C33 alkanes. The US EPA CMB Software
341   version 8.2 was used. Source profiles for vegetative detritus (Rogge et al., 1993), wood burning (Fine et al.,
342   2004), diesel and gasoline motor vehicles (Lough et al., 2007) were included in the final result. In addition, a
343   profile for poorly maintained vehicles ('smoking vehicles') (Lough et al., 2007) was evaluated but found
344   inappropriate. The link between tracers and sources is discussed in further detail in section 3.5.2. The secondary
345   organic aerosol fraction was calculated based on WSOC not related to biomass burning (Sannigrahi et al., 2006).
346   The fitting statistics for the final result are shown in Table 3.

347

3   Results & Discussion

349

3.1   Time Series and Diurnal Cycle

351   The 30 min data time series of O_3, NO_2, NO, CO, benzene, toluene, and PM_{10}, along with basic
352   meteorological data from the BLUME station in Neukölln and MLH as derived from the proprietary software are
353   shown in Figure 2, spanning the duration of the campaign. All times are given in CET. The 8 h mean ozone
354   concentrations show that the EU target value for ozone (120 µg m^{-3} based on 8 h means) was exceeded 6 times
355   during the measurement period, and the WHO guideline (100 µg m^{-3}) was exceeded 18 times. The hourly limit
356   value for NO_2 (200 µg m^{-3}) was not exceeded, though concentrations often exceeded 100 µg m^{-3}. The daily limit
357   value for PM_{10} (50 µg m^{-3}) was not exceeded.

358   Elevated concentrations were often observed at the same time for many of the pollutants included in
359   Figure 2, with the exception of ozone. Ozone, as a secondary pollutant formed photochemically from NOx and
360   NMVOC precursors, follows a similar pattern to temperature (Pearson correlation coefficient [standard error] of
361   0.82 [0.014]), and peaks at different times than the primary pollutants. The formation of ozone can be limited by
362   either NO_x or NMVOCs, depending on the ambient concentrations which are controlled by sources (e.g.,
363   vehicles, biogenics) and transport. NO_2, NO, CO, toluene, and benzene all have diurnal cycles that peak in the
364   morning and evening, reflecting their anthropogenic traffic-related emission sources (see Figure S1 in SI). The
365   morning peak in the pollutants occurred at 7 or 8 am, while the evening peak occurred quite late between 9 and
366   11 pm, likely owing to a combination of daytime emissions and the decrease in the MLH. Traffic counts, from
367   MC143 and MC220 in Neukölln (see location in Figure 1), showed that traffic increased dramatically between 6
368   and 8-9 am, after which a slow but steady increase led to a peak at 5-6 pm, after which the traffic count dropped
369   dramatically. In contrast, ozone, temperature, and mixing layer height followed parallel diurnal cycles with a

370 minimum at 6 am and a broad afternoon peak between noon and 6 pm. During BAERLIN2014 the maximum

371 height of the mixing layer was found to be 1.5-2 km between noon and 18:00 and below 500 m during the

372 night/early morning. These numbers indicate the vertical extent of the urban pollution layer over the

373 measurement site where pollutants are most likely residing. Relative humidity showed the opposite with a peak

374 at 6 am, and a broad low between noon and 6 pm.

375 These results are supported by the Pearson correlation coefficients among NO_2, NO, CO, toluene, and

376 benzene, which for hourly values range from 0.51-0.82 (all statistically significant at an alpha=0.05; see Table

377 S2), with the strongest relationship between CO and NO_2. The correlation to relative humidity was found to be

378 negative for MLH (-0.66 [0.022]), temperature (-0.71 [0.014]), and ozone (-0.76 [0.014]). The pollutant with the

379 strongest relationship to temperature was ozone.

380 The time series of particulate matter mass (PM_{10}), derived PM_1, $PM_{2.5}$, and PM_{10} mass from the

381 GRIMM 1.108 particle number size distribution measurements, total particle number, and particle surface area

382 are shown in Figure 3. While the two PM_{10} time series along with the PM and particle number time series

383 associated to the same instrument (GRIMM 1.108) are most similar, the other total particle number time series

384 do not show significant similarities. This is largely owing to the difference in size fractions measured by the

385 different instruments. Correlation analysis of the pollutant concentrations from Neukölln with MLH values on

386 the basis of averaged diurnal cycles of hourly-mean values (in our case monthly averages during July and

387 August) provided highest correlations with PN for accumulation mode particles (size range 100 – 500 nm) and

388 significant correlations for $PM_{2.5}$ and PM_1 (Schäfer et al., 2015) showing similarities to investigations in

389 Augsburg, Germany (Schäfer et al., 2016) and Beijing, China (Tang et al., 2016). In addition to this

390 investigation for the reference site, a more detailed correlation analysis of the MLH with PM_{10}, O_3, and NO_x

391 taking into account all 16 BLUME stations in Berlin was carried out using the MATLAB approach outlined

392 here, as well as an alternative approach, COBOLT (Geiß et al., 2017). In this context it was assumed that the

393 MLH derived for the reference site in Neukölln is representative for the entire metropolitan area of Berlin. The

394 correlation analysis of the diurnal cycles (averaged over the duration of ceilometer measurements from

395 BAERLIN2014) of the MLH and PM_{10} found that correlations were completely different at the different sites

396 regardless of site type, indicating that surface concentrations of PM_{10} were not predominantly determined by the

397 MLH, but rather by local sources and sinks, and meteorological factors, among others. In the case of O_3, strong

398 positive correlations were identified for both the BLUME sites on the periphery of Berlin, as well as the urban

399 background locations. In contrast, for NO_2, a negative correlation to MLH was observed for all sites at the

400 periphery of the city, and to a lesser extent at some of the urban background sites (Geiß et al., 2017).

401 Particle size distribution during the study period is shown in Figure 4. Size distribution was dominated

402 by ultrafine number size distribution ("UFP", <100 nm) throughout the day (i.e. particle formation close by). The

403 number and volume distribution was further binned into at least 5 size bins, as presented in Figure 4 for

404 comparison with other urban background measurements. The average daytime total number and volume

405 concentration remained in the range of 5.5 - 6.0 x 10^3 cm^{-3} and 11 - 12 μm^3 cm^{-3}, respectively, in contrast to the

406 stronger signal during the nighttime. The mean (median) total number and volume concentration over the entire

407 measurement period was 6.1 x 10^3 cm^{-3} (5.4 x 10^3 cm^{-3}) and 11.8 μm^3 cm^{-3} (9.5 μm^3 cm^{-3}), respectively. Over

408 80% of the total number concentration is ultrafine particles, and the contribution is higher during the nighttime.

409 Volume distribution is largely dominated by the accumulation mode particles which is typical of many urban

410 sites. The number concentrations were similar to other urban stations in Germany (Birmili et al., 2016).

411   The diurnal cycles for total PN for the three instruments covering the smaller particles (excluding the
412   observations from the GRIMM-1.108) have morning and evening peaks, similar to the diurnal cycle for NO_2,
413   indicating a traffic origin. The diurnal cycle for the larger particles, as sampled by the GRIMM-1.108 has a much
414   more dominant early morning peak and mid-afternoon minimum, without the second evening peak.

415   In Figure 5, at least two major contributors to UFP over the course of the day could be identified, in the
416   morning and during the night. The presence of the morning peak is likely due to traffic-related emissions. Such a
417   peak has also been identified in other species, as well as other studies in urban areas (Borsós et al.,
418   2012;Mølgaard et al., 2013). There was a gradual increase in the UFP concentration from late afternoon which
419   continues overnight till early morning hours. This nighttime feature of UFP was observed during weekends as
420   well as on the weekdays. The reasons for this could be that the source contributing to this is something other than
421   or in addition to traffic and may be active or enhanced overnight, the decrease in mixing layer height at night
422   traps the particles in a smaller volume compared to daytime, and/or that night time deposition of particles is
423   lower than daytime owing to higher atmospheric stability. The co-located trace gas measurement showed that the
424   elevated UFP nighttime concentration correlates with toluene, among other gases such as CO. Daily
425   observations also showed occasional and episodic "particle burst" (new particle formation) events for particles in
426   the size range of 10-50 nm, which could be related to fresh plumes or to regional particle formation events.

3.2 NMVOC measurements – Method comparison

429   The results of the four NMVOC measurement methods were compared and contrasted for benzene and
430   toluene. While differences in e.g., instrumentation and measurement technique (mass-to-charge (m/z) ratios vs
431   compounds), inlet location, and time resolution, do not allow for direct comparisons, a comparison can be useful
432   to understand how different or similar the information provided by the various methods can be. A summary of
433   these methods and the compounds measured, including information on the detection limits and sampling times is
434   provided in Table S1.

435   The 30-min data reported from the BLUME network was compared to the PTR-MS data for m/z 79
436   (benzene) and m/z 93 (toluene), as both instruments provide high time-resolution data. The correlations between
437   the two methods were good given the imperfect nature of the comparison, both with Pearson's r values for
438   benzene and toluene of 0.39, significant at the $p<0.05$ level. The lower correlation values were likely owing to a
439   number of factors including the differences in measurement method, and in location of the inlets for each
440   instrument and thereby source influences – one of which was located on the street side of the van at ca. 2.5 m
441   above ground, while the other was located above the measurement container ca. 5 m from the street. The inlet at
442   the street would be influenced more directly by vehicle emissions in comparison to the inlet above the
443   measurement container, which is especially relevant in that the PTR-MS was likely influence by individual
444   vehicles, while this would not be the case for the container measurements. This influence of vehicles on the
445   PTRMS data at higher time resolution is supported by an increase in Pearson's r values with longer averaging
446   times, which reduces the influence of individual vehicles. For 1 h (3 h) average concentrations the r values
447   increase to 0.48 (0.58) and 0.53 (0.71) for benzene and toluene, respectively, all significant at the $p<0.05$ level.
448   Furthermore, the Pearson's r values for the correlations between the BLUME network and the individual
449   canisters were 0.39 (benzene) and 0.83 (toluene), both statistically significant with p-values <0.05, and between
450   BLUME and the cartridge samples 0.51 (toluene) and not significant for benzene. All benzene and toluene
451   measurements are shown in Figure S2.

452   In order to investigate the possibility of identifying molecular structures of PTR-MS derived m/z
453   measurements, a comparison of the continuous measurements of the PTR-MS and intermittent canister samples
454   was also carried out. For a number of cases only one compound quantified from the canister samples matched a
455   specific m/z, while in other cases multiple compounds were quantified in the canister samples that had the same
456   mass. For example, propanal, acetone, n-butane, and 2-methylpropane all have a molecular weight
457   corresponding to m/z 59 (molar weight M_W = 58 g/mole + $M_W(H^+)$ = 1 g/mole), among which the PTR-MS
458   cannot distinguish. In some cases, the fractional contribution of compounds with the same m/z ratio was
459   relatively similar across all canister samples, as for o-xylene, m+p-xylene, and ethylbenzene (m/z 107). However
460   this was rather the exception, with relative contributions more typically showing significant variation among the
461   canister samples (see Figure S3 in the SI). Correlations between the canister samples and PTR-MS results were
462   carried out for 35 m/z values for which at least one compound was quantified in the canister samples. While the
463   absolute r values of the correlations ranged from 0.00016 to 0.63, the correlations were generally quite poor,
464   showing little to no correlation for many of the m/z (only 9 of the 35 m/z values had r values greater than 0.3).
465   While the difference in e.g., inlet locations, likely played a role, these results seem to indicate that the differences
466   in instrument and quantification method result in substantial differences in what is being quantified so that the
467   comparison does not hold real value.
468
469   **3.3 NMVOC Measurements – Characterization of different locations by canister sampling**
470   The average fractional contribution to mixing ratio by compound class for each of the Neukölln,
471   Altlandsberg, Plänterwald sites, the Tiergarten tunnel and the AVUS motorway samples is presented in Figure 6.
472   The number of compounds included in each class was: alkanes (19), alkenes and alkynes (13), aromatics (14),
473   oxygenated (6), and biogenics and their oxidation products (5; referred to as 'biogenics' for simplicity). For a
474   complete list of the compounds and their grouping, see the supplemental information. In the following text and
475   figures two extremely high values for acetone were removed (one sample from the Neukölln station, and one
476   from the Altlandsberg samples). Since these two values were extreme outliers, their origin remains unclear.
477   Therefore we have removed them from the averages and treated them separately. (Text is included in the SI to
478   demonstrate how these two values change the results presented here.) The largest contributions of the quantified
479   VOCs to mixing ratio were from the alkanes (27 - 41 %) and oxygenated (23 - 55 %) compounds. Biogenics
480   were always a minor contribution to mixing ratio, but their contribution was largest in the Plänterwald samples
481   (11 %) and negligible at the two traffic locations. Alkenes/alkynes and aromatics showed the largest contribution
482   to mixing ratio at the traffic sites, at 17 - 23 % and 14 %, respectively. The highest total NMVOC mixing ratio of
483   those compounds measured here was found at the traffic sites (Tiergarten tunnel, 64 ± 17 ppbv; AVUS
484   motorway, 170 ± 82 ppbv; average mixing ratio ± standard deviation among the samples). The total mixing
485   ratios of the 57 measured compounds at Altlandsberg and at the urban background station in Neukölln, showed
486   similar results, with an average mixing ratio and standard deviation of 14 ± 6.4 ppbv and 19 ± 5.6 ppbv,
487   respectively. The mixing ratios found in Plänterwald were similar to the urban background location, with an
488   average of 17 ± 3.4 ppbv, although with a larger contribution from biogenics. In comparison, total NMHC
489   mixing ratios for urban background in Paris during the MEGAPOLI winter campaign was 12 ppbv (midnight
490   median levels) or 17 ppbv (maximum of median daily values), with somewhat lower mixing ratios measured
491   during the summer campaign (Dolgorouky et al., 2012;Ait-Helal et al., 2014).

492   Previously, a measurement campaign was carried out during June-August of 1996 in Berlin, during

493 which samples were taken at the Neukölln urban background station, as well as at a traffic station on Frankfurter

494 Allee. During this campaign, VOC measurements were taken 4 times a day for 2 hours over the course of one

495 week (7 days) of each month using bag samples, adsorption tubes and DNPH cartridges and analyzed by gas-

496 chromatography (Thijsse et al., 1999). This provides a good basis for comparison to the NMVOCs measured by

497 canister sampling (most similar in method) during this campaign almost 20 years later. Overall, the mixing ratios

498 for most compounds that were measured in both projects at the urban background location in Neukölln were

499 lower now than in 1996 (Figure 7). For the traffic locations the results are less clear. Given that the Frankfurter

500 Allee monitoring station is a traffic station, these measurements would likely be more comparable to the

501 Tiergarten Tunnel measurements of this study, rather than those samples taken during a traffic jam on the AVUS

502 motorway where concentrations were extremely elevated. Indeed, the mixing ratios measured during the traffic

503 jam were found to be higher in most cases than those measured in 1996 at Frankfurter Allee. However, the

504 comparison between the Tiergarten Tunnel measurements and Frankfurter Allee showed much more similar

505 results to those of the urban background station comparison, with concentrations generally being lower today

506 than ca. 20 years ago (Thijsse et al., 1999).

507

3.4 OH Reactivity

509   To better understand the role of these compounds with respect to their role in ozone formation and

510 atmospheric reactivity, the reactivity with respect to OH (R_{OH}) was calculated. These results are shown in Figure

511 6 and parallel the results presented for the mixing ratios. In all cases, including other studies discussed, the

512 values presented are calculated OH reactivity based on measurements of NMVOCs and not OH reactivity that

513 was measured directly. The relative importance of the biogenics, alkenes and alkynes, and to a lesser extent the

514 aromatics increased when considering OH reactivity as is visible in Figure 6 (for a complete list of compounds

515 included in these classes, see the SI). The largest contribution to OH reactivity was from either the biogenics and

516 their oxidation products (0-75%) or the alkenes and alkynes (10-55%), depending on the location, with the

517 alkenes and alkynes dominating at the traffic locations, where the biogenic contribution was negligible. The

518 NMVOCs included in each of these categories are provided in Table S1. The contribution to OH reactivity from

519 alkanes ranged from 4% (Plänterwald) to 18% (AVUS motorway). While the contribution from oxygenated

520 compounds, despite their substantial contribution to mixing ratio, ranged from only 5-13% of OH reactivity.

521 Furthermore, the contribution to the biogenic OH reactivity at Plänterwald originated largely from isoprene

522 (88%), with 7% from α- and β-pinene. Similar contributions were found at Neukölln and Altlandsberg. The

523 mean (median [25th, 75th percentile]) total OH reactivity from the 57 species was 2.6 s^{-1} (2.6 [2.1, 3.0] s^{-1}) at

524 Neukölln, and ranged from 2.2 s^{-1} (2.2 [1.5, 2.8] s^{-1}) at Altlandsberg to 34 s^{-1} (34 [29, 39] s^{-1}) from the AVUS

525 motorway.

526   An earlier study (BERLIOZ) also made measurements of C_2-C_{12} NMHCs in Berlin and at sites in the

527 surrounding area, mostly focused on the production of ozone in downwind locations of the city (Winkler et al.,

528 2002;Volz-Thomas et al., 2003;Becker et al., 2002). They report OH reactivity for two sites outside of Berlin,

529 Blossin (ca. 15-20 km southeast of the Berlin city boundary) and Pabsthum (ca. 30-35 km northwest of the

530 Berlin city boundary). The total OH reactivity reported at these sites range between 1 - 7 sec^{-1} and ca. 0.25 - 2

531 sec^{-1}, respectively. These are similar to those values found at the urban background locations in Berlin, with the

532 most comparable location being Altlandsberg (2.2 s^{-1}). The contribution from isoprene to the OH reactivity was

533 found to be 70% at Blossin and 51% at Pabstthum, on average, although during the passing of a city plume at

534 Pabsthum 46% of reactivity was contributed by isoprene, with the remaining contribution attributed to

535 anthropogenic NMHCs (Winkler et al., 2002).

536   The total OH reactivity values of measured VOCs in Berlin (2.6 s^{-1}) are similar to the average total OH

537 reactivity from VOCs observed in other European cities, such as Paris (ca. 4.0 s^{-1}) and London (1.8 s^{-1})

538 (Dolgorouky et al., 2012;Whalley et al., 2016), and, not surprisingly, lower than those observed at cities in the

539 Pearl River Delta region of China (8-14 s^{-1}). Specifically, Liu et al. (2008) reported OH reactivity from a

540 measurement campaign in Ghangzhou and Xinken during one month in the autumn of 2004. The OH reactivity

541 from alkanes, alkenes, and aromatics from Ghangzhou was reported to be 1.9 ± 1.5 s^{-1}, 8.8 ± 6.8 s^{-1}, and 2.9 ±

542 2.7 s^{-1}, respectively. In all cases, these values are about one order of magnitude greater than those calculated for

543 the urban background locations during this campaign (see Table 2). The level for isoprene (0.5 ± 0.4 s^{-1})

544 however, was much more similar to the OH reactivity reported for the biogenics at the urban background

545 locations in this study. In London, OH reactivity of alkanes, alkenes+alkynes, aromatics, and biogenics was

546 reported to be 0.81 s^{-1}, 0.47 s^{-1}, 0.235 s^{-1}, and 0.25 s^{-1}, respectively, which are values much more similar to those

547 in this study (Whalley et al., 2016). The relative importance of alkanes and alkenes+alkynes was the reverse for

548 London compared to Berlin.

549   In the MEGAPOLI winter campaign in Paris, total calculated mean OH reactivity was reported to be

550 17.5 s^{-1}, although this included not only NMVOCs, but also methane, CO, NO, and NO$_2$ (Dolgorouky et al.,

551 2012). The OH reactivity attributed to the 29 non-methane hydrocarbons and oxygenated VOCs was 23% (4.0 s^{-1}

552) of the total, somewhat higher than those values reported here (57 NMVOCs) for the urban background

553 locations. Comparing to the OH reactivity values in Berlin is difficult, since for the winter campaign in Paris,

554 Ait-Helal et al. (2014) report that the concentrations of the VOCs are generally shown to be lower during

555 summer, specifically for many of the anthropogenic compounds, although this does vary by compound.

556 Therefore, the OH reactivity values for Paris considered here should be considered an upper limit for the

557 comparison with this study. The calculated mean OH reactivity attributed to NO and CO was 1.75 s^{-1} each, and

558 9.63 s^{-1} for NO$_2$ in Paris (Dolgorouky et al., 2012). By comparison, the mean OH reactivity calculated for

559 August (to match the time during which the canister samples were taken at Neukölln) was 0.58 ± 1.2 s^{-1} and 0.87

560 ± 0.30 s^{-1} for NO and CO, respectively, and 4.5 ± 3.0 s^{-1} for NO$_2$, which is again, lower, as with the VOCs, but

561 not unreasonable given the context of the comparison.

562

3.4.1   OH reactivity – direct comparison to a previous study in London and Paris

564   As a comparison to the R$_{OH}$ estimates calculated for London and Paris based on ca. 10 years of

565 monitoring data through 2009 (von Schneidemesser et al., 2011), a subset of the NMVOCs was taken to enable a

566 more equal comparison to the values reported for summer (JJA) in that study. The only difference in the

567 compounds included is the contribution of n-butane, which was not included in the Berlin calculations because

568 of a local source of contamination (in London the contribution of n-butane to OH reactivity from this subset of

569 NMVOCs was ca. 5% or less). The referenced study was focused on the contribution of biogenics, specifically

570 isoprene, to OH reactivity. At the London Eltham site (urban background) isoprene contributed 25% to the OH

571 reactivity for summer and 16% at Paris Les Halles, also an urban background location (24 total NMVOCs,

572 including 9 alkanes, 9 alkenes/alkynes, 5 aromatics, 0 oxygenated, 1 biogenic) (von Schneidemesser et al.,

573 2011). Using the reduced, matched set of compounds, isoprene accounts for 37% of OH reactivity at the

574 Neukölln location on average, and as much as 82% at the Plänterwald (urban park) location in Berlin. The
575 Neukölln urban background location values are a bit higher than those in London and Paris, although not
576 dramatically different. The Plänterwald urban park location however, demonstrates the importance of such areas
577 for the biogenic influence on OH reactivity, especially considering that even at Harwell, a rural background
578 location west of London in the UK, isoprene contributes on average only 10% of OH reactivity. Although, as
579 pointed out in the study, this is likely an underestimation of the biogenic importance given that only isoprene is
580 included and for northerly regions other biogenics, such as monoterpenes may play a more important role (von
581 Schneidemesser et al., 2011).

582

583 **3.5 PM₁₀ Filters**

584 **3.5.1   Bulk composition and HYSPLIT back trajectories**

585 The PM₁₀ filters were analyzed for water soluble and water insoluble OC, EC, and ions. In addition,
586 filter samples were grouped to ensure enough mass for analysis of organic molecular markers. The groups were
587 informed by the bulk composition analysis results, including the ratio of water soluble to total OC and the ratio
588 of ions to OC, and HYSPLIT back trajectories. The results of this bulk composition analysis are shown in Figure
589 8. Select individual filters that had sufficient mass and did not fit with any of the other groups were analyzed
590 individually (B17, B19, B30). All values listed for groups are an average of the results from the filters included
591 in the group. The air mass origin as per HYSPLIT are summarized in Table 3 (see also Figure S4).

592 Groups A, B, C, and D show significant similarity in their percent of OC that is WSOC, which ranges
593 from 27 to 34%. The ratio of ions (sulfate, nitrate, ammonium) to OC is however, very different. Groups B and C
594 have an ions:OC ratio of 1.2 and 0.98, while groups A and D have ratios of 0.56 and 0.50, respectively. The
595 PM₁₀ mass loadings for B (20 µg m⁻³) and C (24 µg m⁻³) were lower than for A (27 µg m⁻³) and D (35 µg m⁻³),
596 see Table 3. The back trajectories (Figure S4) show that prior to arriving in Berlin, the air masses primarily
597 passed over Germany for group A. While some additional filters fit the general patterns outlined here, the
598 number of filters included in the group was reduced to focus more on back trajectories in the group that
599 originated from over Germany itself. The air masses that characterize group D originated from the Northeast,
600 passing over the Baltic coast and Poland before arriving in Berlin. For group B the air masses originated from
601 the West over the Atlantic (not further than 20 degrees W) and passed over northern France, the BeNeLux region
602 and central Germany before arriving in Berlin. For group C, the air masses originated from the North West, over
603 the North Sea as far as Iceland, passing between the UK and the Scandinavian Peninsula before arriving in
604 Berlin. Both B and C had higher concentrations of sodium and nitrate than A and D, while A and D had higher
605 concentrations of OC and marginally higher concentrations of sulfate than B and C (Figure 8). The
606 concentrations of EC ranged between 1.1 and 1.9 µg m⁻³ but did not group as with the other species, with the
607 lowest concentration in group B and the highest in group C.

608 Group E had a very low percent of WSOC (19%) and an ions:OC ratio of 0.59. It also had the lowest
609 PM₁₀ mass (20 µg m⁻³), and either the lowest or among the lowest concentrations for all ions. The OC
610 concentration however, was 5.5 µg m⁻³, which was roughly in the middle of the OC concentrations measured,
611 while the EC concentration was also the lowest at 0.71 µg m⁻³. The air masses originated from the North, passing
612 over Scandinavia, the North Sea, or the UK before arriving in Berlin.

613 B17, B19, and B30 were analyzed individually because their bulk composition analysis and back
614 trajectory patterns did not group well with the others, and sufficient mass was available for tracer analysis

615   without needing to composite filters (Table 3, Figure 8). B17 and B30 had a higher percent WSOC (66% and

616   56%, respectively), and ions:OC ratios of 1.3 and 2.4, respectively. 37% of OC was WSOC for B19, and the

617   ions:OC ratio was 0.77. Total PM_{10} mass was 38.8 µg m^{-3}, 31.0 µg m^{-3}, and 39.5 µg m^{-3}, and OC concentrations

618   were 7.0 µg m^{-3}, 5.9 µg m^{-3}, and 3.9 µg m^{-3}, for B17, B19, and B30, respectively. All three samples had

619   significantly larger contributions from sulfate, and to a lesser extent also higher ammonium, compared to the

620   other groups. The back trajectories associated with B17 and B19 both passed over Poland before arriving in

621   Berlin, with the air masses associated with B19 extending more northward as well. For B30 the air originates

622   from the West with some passing over northern France, but mostly comes from over Germany itself. The

623   significant presence of ammonium and sulfate likely indicates influence of agriculture, as ammonium sulfate is

624   commonly used in fertilizer and more than 95% of NH_3 emissions in Europe originate from agriculture (Harrison

625   and Webb, 2001;Backes et al., 2016;EEA, 2016). B30 also has a large amount of nitrate in contrast to all other

626   samples, and somewhat higher concentrations of potassium and sodium as well. B17 had the highest

627   concentration of EC (2.3 µg m^{-3}) of all samples.

628   There were significant concentrations of sulfate across all samples, ranging from 1.2-6.0 µg m^{-3}, but

629   particularly so in B17, B19, and B30. Sulfate is typically attributed to industrial sources, as the content of sulfate

630   in fuels has been reduced significantly and is now quite low (Villalobos et al., 2015). Sea-salt is in this case not

631   likely as a source, as Berlin is not within close proximity of a coastal region where such components are

632   typically identified (Putaud et al., 2004). In general the significant contributions of sulfate, nitrate, and

633   ammonium are indicative of a secondary inorganic aerosol (ammonium sulfate and ammonium nitrate) (Putaud

634   et al., 2004;Schauer et al., 1996). Previous work has shown that secondary inorganic aerosol over northwestern

635   Europe, including Germany, contribute significantly – about 50% – to the PM_{10} concentrations (Banzhaf et al.,

636   2013). Two studies by Putaud et al. (Putaud et al., 2004;Putaud et al., 2010) summarize the relative contribution

637   of major constituent chemical species to PM mass, including for near-city and urban background locations. In

638   comparison to the numbers cited in that study (2004 all European sites; 2010 north-western European sites), the

639   percent contribution of nitrate (15%; 14%), ammonium (7%; not listed), and sulfate (13%; 14%) to PM_{10} mass at

640   the urban background site in Berlin were quite similar, ranging from 1-11% (nitrate), 1-5% (ammonium), and 6-

641   16% (sulfate) in Berlin.

642

643   **3.5.2   Organic molecular markers**

644   The concentrations by composited sample are shown in Figure 9 for the organic molecular markers.

645   Levoglucosan has been established as a molecular marker for biomass burning (Simoneit et al., 1999). The

646   concentrations measured here ranged from 15-60 ng m^{-3}. While high concentrations of levoglucosan in urban

647   areas are often associated with residential wood combustion during colder months, it can also be owing to crop

648   burning, wild fires, coal combustion and/or long-range transport of smoke from biomass burning (Simoneit,

649   2002;Zhang et al., 2008;Shen et al., 2016). The concentrations measured during this summer campaign in Berlin

650   were similar to those measured in PM_{10} from other European cities during summertime, and ca. an order of

651   magnitude lower than concentrations observed in winter (Caseiro and Oliveira (2012) and references therein).

652   The study by Caseiro and Oliveira (2012) confirms the likelihood of agricultural residue burning and/or wildfires

653   as a summertime source for levoglucosan.

654   Alkanes are useful tracers to distinguish between fossil fuel sources and vegetative detritus. This

655   distinction is informed by the odd-even carbon number predominance, specifically of the C_{29}, C_{31}, and C_{33} *n-*

alkanes to indicate plant material as a source (Rogge et al., 1993). As is visible in Figure 9, the concentrations of those odd *n*-alkanes are much greater than the corresponding even *n*-alkanes. Furthermore, the carbon preference index (CPI) was calculated for the samples using the C_{29}-C_{33} *n*-alkanes and ranged from 1.9-5.5, with an average of 3.6. CPI values of ca. 1 are indicative of fossil fuel emission sources, whereas values of ca. 2 or greater are indicative of biogenic detritus (Simoneit, 1986), as is clearly the case for these samples.

Hopanes have been established as markers for diesel and gasoline vehicle emissions, stemming from petroleum product utilization and lubricating oil used in vehicles (Schauer et al., 1996;Rushdi et al., 2006;Simoneit, 1984). The concentrations of the two hopanes measured here and included in the CMB analysis ranged from 0.04-0.13 ng m^{-3} as shown in Figure 9.

Polycyclic aromatic hydrocarbons (PAHs) are formed and emitted most typically during the incomplete combustion of fossil fuels or wood (Ravindra et al., 2008). The concentrations measured during this study ranged from 0-0.23 ng m^{-3} for the individual PAHs shown in Figure 9. These concentrations are similar to, although on the lower end, of those measured in a study in Flanders, Belgium, including measurements at urban locations (Ravindra et al., 2006). Generally, PAH concentrations are lower in summertime owing to lower emissions and shorter lifetimes. The measurements here were conducted during summer, while the measurements in the study in Flanders covered more seasons. To distinguish between sources, PAH concentration profiles or ratios are used. For example, a ratio of benzo(b)fluoranthene to benzo(k)fluoranthene of greater than 0.5 has been identified as an indicator for diesel emissions sources (Park et al., 2002;Ravindra et al., 2008). In this study the ratio ranged from 1.9 to 7.2, indicating a strong influence of diesel emissions for these compounds.

3.5.3   Chemical Mass Balance

The molecular markers analyzed in the organic carbon fraction of the PM$_{10}$ samples were used to conduct source apportionment analysis using chemical mass balance. The total OC for these samples ranged from 2.99 to 7.21 μg m^{-3}. The amount of OC mass apportioned in the CMB analysis ranged from 21% to 49%. The source profiles included in the model to which OC was attributed includes vegetative detritus, diesel emissions, gasoline vehicle emissions, and wood burning. In addition, a fraction of the unapportioned OC was attributed to secondary organic aerosol based on the unapportioned fraction of water soluble OC and the amount attributed to wood burning, following Sannigrahi et al. (2006). The source contributions to OC, as well as the fitting statistics are listed in Table 4, and shown in Figure 10.

For B17, B19, and B30 the SOA fraction is higher than for any of the others, at 63%, 34%, and 49% of OC, respectively. They also had the highest concentrations of levoglucosan, ranging from 37.8 to 60.1 ng m^{-3}. As the primary tracer for biomass burning, these three samples also had the largest concentrations attributed to this source, ranging from 0.22 to 0.44 μg m^{-3} of OC, but the relative contribution was only larger for B30 at 11%. All other samples had contributions that ranged between 2% and 4% of OC. These three samples had air masses that originated over Poland (B17, B19) and Germany (B30), indicating a more local-regional source for the biomass burning. The higher concentrations of potassium in these samples, also an indicator for biomass burning (Andreae, 1983), provides additional confirmation. The relatively high concentrations of ammonium and sulfate in these samples may indicate an agricultural influence. Those samples originating from regions to the West/North had somewhat lower concentrations overall relative to those originating from regions to the East/North, as shown in Figure 10.

The contribution of diesel emissions ranged from 0.24 - 0.81 µg m^{-3}, corresponding to 4 - 21% of OC fraction. The highest fractional contribution was found in GRC (concentration 0.74 µg m^{-3}) (air masses originating over the North Sea), while the highest concentration was found in sample B17 (fractional contribution 12%) (from Poland to the East). The diesel from GRC could also have its origin in shipping emissions, as well as diesel vehicles. High contributions of diesel did not necessarily correspond to high contributions of gasoline vehicle emissions, which were lower than the contributions from diesel and ranged from 0.11 - 0.28 µg m^{-3} and 2 - 7% of OC. The highest contribution in terms of fractional contribution and concentration was found in B30.

The contribution of vegetative detritus was among the largest source contributions and ranged from 0.51 - 1.4 µg m^{-3} (11-20%). The relative importance of this source is reflected in the concentrations of the alkanes, as shown in Figure 9, and their average CPI of 3.6. The largest contribution was found for GRD with air masses originating over the North Sea.

For all samples, a significant amount of secondary organic aerosol was calculated, 0.87 - 4.4 µg m^{-3} (18 - 63%). While this was the contribution to OC, high concentrations of inorganics (sulfate, ammonium, nitrate) support this significant contribution from secondary aerosol overall.

3.5.4 Source apportionment – emission inventory comparison

The source apportionment results were compared to the emissions inventory (EI) from TNO-MACC III (Kuenen et al., 2014). The grid cells for Berlin were extracted and the percent of total emissions for OC by source category for the Berlin area for June, July, and August as a rough comparison to the source apportionment results was calculated. Both diesel and gasoline vehicle exhaust sources have significant contributions, although diesel contributes ca. 19% to total OC emissions in the inventory, whereas gasoline vehicles contribute only about 1%. Biogenic sources are not included in the inventory. If we focus on the primary sources from the source apportionment results, the diesel and gasoline vehicles contribute a significant fraction, with diesel comprising a larger fraction than gasoline vehicles, as in the inventory. The inventory also includes significant contributions from road transport originating from road, brake, and tire wear, which are not reflected in the CMB results, owing to the profiles used. About 8% of OC emissions are attributed to agriculture in the EI. This could contribute to both the biomass burning and vegetative detritus sources; the presence of significant secondary ammonium and nitrate also indicates an agricultural influence, even though this does not show up in the OC CMB. In all cases, these primary sources will contribute to secondary inorganic and organic aerosol formation. The contributions from non-industrial combustion and energy and other industries are not captured as primary source contributions in the CMB model. Overall, the comparison between the source apportionment results and the EI is a non-ideal comparison given the differences in methodology and the difference in terms of primary vs secondary sources that are or are not included. More specifically, the EI provides primary emissions estimates for a year for all Berlin grid cells (Kuenen et al., 2014), while the CMB results provide source attribution to ambient concentrations including primary and secondary sources for 3 months of summer at one location in Berlin. However, one would expect that general patterns are captured for significant sources, as it was for vehicle emissions, and the indication of agriculture.

4 Conclusions

The data presented here provide an overview of the stationary measurements conducted during the BAERLIN2014 campaign. Of the three main aims of the campaign, two were addressed here, including (1) characterization of gaseous and particulate pollution, including source attribution, in the Berlin-Potsdam area, (2) quantification of the role of natural sources, especially vegetation, in determining levels of gaseous pollutants such as ozone. PM_{10} concentrations and the contributions from inorganic species, such as nitrate, sulfate, and ammonium that contribute substantially (10-24%) to secondary aerosol were found to be similar in terms of their relative contribution to PM_{10} in other European cities. Both the PM and gas-phase pollutants exhibited diurnal cycles indicative of anthropogenic sources, and the ratio of benzene to toluene indicated the influence of fresh, local emissions. Comparison of canister samples taken over the course of a day showed similarities which would seem to imply an urban background level for many NMVOC species. In addition to the secondary inorganic aerosol, a significant fraction of OC was attributed to secondary organic aerosol (18-63%) in the CMB analysis.

The influence of vegetation and biogenic emissions was demonstrated in the canister sample analysis, as well as the CMB results where vegetative detritus comprised one of the larger sources contributing to the OC fraction ranging from 11 to 20%. While the detected mixing ratios of the biogenic NMVOCs did not contribute significantly to the total NMVOC mixing ratio, the role in e.g., ozone formation, assessed by calculating OH reactivity, was much more significant. Biogenics and their oxidation products accounted for 31% of the OH reactivity at the urban background station in Neukölln and 75% at the urban park location (Plänterwald), demonstrating the importance of urban parks for biogenic emissions. These contributions from biogenics were higher than those found at comparable urban background locations in London and Paris. This is likely linked to the relatively high amount of land surface area in Berlin which is covered by vegetated areas (34%).

As an outlook, future research could build on this work to include additional analysis of PTR-MS data using positive matrix factorization to investigate the sources influencing NMVOC concentrations at the Neukölln location, as well as modeling studies to gain greater insight as to the impact of urban vegetation on ozone formation, both yielding further insight into the importance of biogenic VOCs in urban environments.

5   Data availability

The datasets generated during and/or analysed during the current study are available from the corresponding author on request.

6   Acknowledgements

This work was hosted by IASS Potsdam, with financial support provided by the Federal Ministry of Education and Research of Germany (BMBF) and the Ministry for Science, Research and Culture of the State of Brandenburg (MWFK). The authors would like to thank Hugo Denier van der Gon and Jeroen Kuenen (TNO) for providing information pertaining to the TNO-MACCIII inventory and Friderike Kuik for the Berlin emissions processing; Christoph Münkel from Vaisala GmbH, Hamburg for support with ceilometer CL51 data analyses to determine mixing layer heights; Wolfram Birmili (UBA), Alfred Wiedensohler, and Kay Weinhold (TROPOS) for discussions informing the particle measurements, colleagues at the IASS for their support of the campaign and discussions that helped shape the manuscript. The authors gratefully acknowledge the NOAA Air Resources Laboratory (ARL) for the provision of the HYSPLIT transport and dispersion model and/or READY website (http://www.ready.noaa.gov) used in this publication. Boris Bonn highly acknowledges a grant from the IASS to support the studies.

777

7   References

779   Ait-Helal, W., Borbon, A., Sauvage, S., de Gouw, J. A., Colomb, A., Gros, V., Freutel, F., Crippa, M., Afif, C.,
780   Baltensperger, U., Beekmann, M., Doussin, J. F., Durand-Jolibois, R., Fronval, I., Grand, N., Leonardis, T.,
781   Lopez, M., Michoud, V., Miet, K., Perrier, S., Prévôt, A. S. H., Schneider, J., Siour, G., Zapf, P., and Locoge,
782   N.: Volatile and intermediate volatility organic compounds in suburban Paris: variability, origin and importance
783   for SOA formation, Atmos. Chem. Phys., 14, 10439-10464, 10.5194/acp-14-10439-2014, 2014.

784   Andreae, M. O.: Soot carbon and excess fine potassium: long-range transport of combustion-derived aerosols,
785   Science (New York, N.Y.), 220, 1148-1151, 10.1126/science.220.4602.1148, 1983.

786   Backes, A. M., Aulinger, A., Bieser, J., Matthias, V., and Quante, M.: Ammonia emissions in Europe, part II:
787   How ammonia emission abatement strategies affect secondary aerosols, Atmos. Environ., 126, 153-161,
788   http://dx.doi.org/10.1016/j.atmosenv.2015.11.039, 2016.

789   Banzhaf, S., Schaap, M., Wichink Kruit, R. J., Denier van der Gon, H. A. C., Stern, R., and Builtjes, P. J. H.:
790   Impact of emission changes on secondary inorganic aerosol episodes across Germany, Atmos. Chem. Phys., 13,
791   11675-11693, 10.5194/acp-13-11675-2013, 2013.

792   Becker, A., Scherer, B., Memmesheimer, M., and Geiß, H.: Studying the city plume of Berlin on 20 July 1998
793   with three different modelling approaches, Journal of Atmospheric Chemistry, 42, 41-70,
794   10.1023/A:1015776331339, 2002.

795   Birmili, W., Weinhold, K., Rasch, F., Sonntag, A., Sun, J., Merkel, M., Wiedensohler, A., Bastian, S., Schladitz,
796   A., Löschau, G., Cyrys, J., Pitz, M., Gu, J., Kusch, T., Flentje, H., Quass, U., Kaminski, H., Kuhlbusch, T. A. J.,
797   Meinhardt, F., Schwerin, A., Bath, O., Ries, L., Gerwig, H., Wirtz, K., and Fiebig, M.: Long-term observations
798   of tropospheric particle number size distributions and equivalent black carbon mass concentrations in the
799   German Ultrafine Aerosol Network (GUAN), Earth Syst. Sci. Data, 8, 355-382, 10.5194/essd-8-355-2016, 2016.

800   Blake, R. S., Monks, P. S., and Ellis, A. M.: Proton-Transfer Reaction Mass Spectrometry, Chemical Reviews,
801   109, 861-896, 10.1021/cr800364q, 2009.

802   Bonn, B., von Schneidemesser, E., Andrich, D., Quedenau, J., Gerwig, H., Lüdecke, A., Kura, J., Pietsch, A.,
803   Ehlers, C., Klemp, D., Kofahl, C., Nothard, R., Kerschbaumer, A., Junkermann, W., Grote, R., Pohl, T., Weber,
804   K., Lode, B., Schönberger, P., Churkina, G., Butler, T. M., and Lawrence, M. G.: BAERLIN2014 – the influence
805   of land surface types on and the horizontal heterogeneity of air pollutant levels in Berlin, Atmos. Chem. Phys.,
806   16, 7785-7811, 10.5194/acp-16-7785-2016, 2016.

807   Borsós, T., Řimnáčová, D., Ždímal, V., Smolík, J., Wagner, Z., Weidinger, T., Burkart, J., Steiner, G., Reischl,
808   G., Hitzenberger, R., Schwarz, J., and Salma, I.: Comparison of particulate number concentrations in three
809   Central European capital cities, Science of The Total Environment, 433, 418-426,
810   http://dx.doi.org/10.1016/j.scitotenv.2012.06.052, 2012.

811   Bourtsoukidis, E., Williams, J., Kesselmeier, J., Jacobi, S., and Bonn, B.: From emissions to ambient mixing
812   ratios: Online seasonal field measurements of volatile organic compounds over a Norway spruce-dominated
813   forest in central Germany, Atmospheric Chemistry and Physics, 14, 6495-6510, 10.5194/acp-14-6495-2014,
814   2014.

815   Brauer, M., Freedman, G., Frostad, J., van Donkelaar, A., Martin, R. V., Dentener, F., Dingenen, R. v., Estep,
816   K., Amini, H., Apte, J. S., Balakrishnan, K., Barregard, L., Broday, D., Feigin, V., Ghosh, S., Hopke, P. K.,
817   Knibbs, L. D., Kokubo, Y., Liu, Y., Ma, S., Morawska, L., Sangrador, J. L. T., Shaddick, G., Anderson, H. R.,
818   Vos, T., Forouzanfar, M. H., Burnett, R. T., and Cohen, A.: Ambient Air Pollution Exposure Estimation for the
819   Global Burden of Disease 2013, Environmental Science & Technology, 50, 79-88, 10.1021/acs.est.5b03709,
820   2016.

821   Caseiro, A., and Oliveira, C.: Variations in wood burning organic marker concentrations in the atmospheres of
822   four European cities, Journal of environmental monitoring : JEM, 14, 2261-2269, 10.1039/c2em10849f, 2012.

823   Colette, A., Bessagnet, B., Vautard, R., Szopa, S., Rao, S., Schucht, S., Klimont, Z., Menut, L., Clain, G.,
824   Meleux, F., Curci, G., and Rouïl, L.: European atmosphere in 2050, a regional air quality and climate perspective
825   under CMIP5 scenarios, Atmos. Chem. Phys., 13, 7451-7471, 10.5194/acp-13-7451-2013, 2013.

826   Derwent, R. G.: New Directions: Prospects for regional ozone in north-west Europe, Atmos. Environ., 42, 1958-
827   1960, 2008.

828 Dolgorouky, C., Gros, V., Sarda-Esteve, R., Sinha, V., Williams, J., Marchand, N., Sauvage, S., Poulain, L.,
829 Sciare, J., and Bonsang, B.: Total OH reactivity measurements in Paris during the 2010 MEGAPOLI winter
830 campaign, Atmos. Chem. Phys., 12, 9593-9612, 10.5194/acp-12-9593-2012, 2012.

831 EC: Directive 2008/50/EC of the European Parliament and of the Council of 21 May 2008 on ambient air quality
832 and cleaner air for Europe, in: 2008/50/EC, edited by: Union, E. P. a. t. C. o. t. E., Official Journal of the
833 European Union, 2008.

834 EEA: Air quality in Europe - 2016 report, European Environment Agency, Luxembourg, 2016.

835 Ehlers, C.: Mobile Messungen: Messung und Bewertung von Verkehrsemissionen, PhD, Mathematisch-
836 Naturwissenschaftliche Fakultät, Universität Köln, 2013.

837 Ehlers, C., Klemp, D., Rohrer, F., Mihelcic, D., Wegener, R., Kiendler-Scharr, A., and Wahner, A.: Twenty
838 years of ambient observations of nitrogen oxides and specified hydrocarbons in air masses dominated by traffic
839 emissions in Germany, Faraday Discussions, 189, 407-437, 10.1039/C5FD00180C, 2016.

840 Emeis, S., Jahn, C., Münkel, C., Münsterer, C., and Schäfer, K.: Multiple atmospheric layering and mixing-layer
841 height in the Inn valley observed by remote sensing, Meteorologische Zeitschrift, 16, 415-424, 10.1127/0941-
842 2948/2007/0203, 2007.

843 Emeis, S., Schäfer, K., and Münkel, C.: Surface-based remote sensing of the mixing-layer height a review,
844 Meteorologische Zeitschrift, 17, 621-630, 10.1127/0941-2948/2008/0312, 2008.

845 Fine, P. M., Cass, G. R., and Simoneit, B. R. T.: Chemical Characterization of Fine Particle Emissions from the
846 Fireplace Combustion of Wood Types Grown in the Midwestern and Western United States, Environmental
847 Engineering Science, 21, 387-409, 10.1089/109287504323067021, 2004.

848 Geels, C., Andersson, C., Hänninen, O., Lansø, A., Schwarze, P., Skjøth, C., and Brandt, J.: Future Premature
849 Mortality Due to O3, Secondary Inorganic Aerosols and Primary PM in Europe — Sensitivity to Changes in
850 Climate, Anthropogenic Emissions, Population and Building Stock, International Journal of Environmental
851 Research and Public Health, 12, 2837, 2015.

852 Geiß, A., Wiegner, M., Bonn, B., Schäfer, K., Forkel, R., von Schneidemesser, E., Münkel, C., Chan, K. L., and
853 Nothard, R.: Mixing layer height as an indicator for urban air quality?, Atmospheric Measurement Techniques,
854 10, 2969-2988, 10.5194/amt-10-2969-2017, 2017.

855 Gilman, J. B., Kuster, W. C., Goldan, P. D., Herndon, S. C., Zahniser, M. S., Tucker, S. C., Brewer, W. A.,
856 Lerner, B. M., Williams, E. J., Harley, R. A., Fehsenfeld, F. C., Warneke, C., and de Gouw, J. A.: Measurements
857 of volatile organic compounds during the 2006 TexAQS/GoMACCS campaign: Industrial influences, regional
858 characteristics, and diurnal dependencies of the OH reactivity, Journal of Geophysical Research: Atmospheres,
859 114, n/a-n/a, 10.1029/2008JD011525, 2009.

860 Goldan, P. D., Kuster, W. C., Williams, E., Murphy, P. C., Fehsenfeld, F. C., and Meagher, J.: Nonmethane
861 hydrocarbon and oxy hydrocarbon measurements during the 2002 New England Air Quality Study, J. Geophys.
862 Res., 109, D21309, doi:10.1029/2003JD004455, 2004.

863 Görner, P., Simon, X., Bémer, D., and Lidén, G.: Workplace aerosol mass concentration measurement using
864 optical particle counters, Journal of Environmental Monitoring, 14, 420-428, 2012.

865 Harrison, R., and Webb, J.: A review of the effect of N fertilizer type on gaseous emissions, in: Advances in
866 Agronomy, Academic Press, 65-108, 2001.

867 Heim, M., Kasper, G., Reischl, G. P., and Gerhart, C.: Performance of a New Commercial Electrical Mobility
868 Spectrometer, Aerosol Science and Technology, 38, 3-14, 10.1080/02786820490519252, 2004.

869 Helsper, C., Horn, H.-G., Schneider, F., Wehner, B., and Wiedensohler, A.: Intercomparison of five mobility
870 size spectrometers for measuring atmospheric submicrometer aerosol particles, Partikelmesstechnik, 68, 475-
871 481, 2008.

872 Jacob, D. J., and Winner, D. A.: Effect of climate change on air quality, Atmos. Environ., 43, 51-63,
873 10.1016/j.atmosenv.2008.09.051, 2009.

874 Kaminski, H.: personal communication, in, edited by: Gerwig, H., 2011.

875 Kaminski, H., Kuhlbusch, T. A. J., Rath, S., Götz, U., Sprenger, M., Wels, D., Polloczek, J., Bachmann, V.,
876 Dziurowitz, N., Kiesling, H.-J., Schwiegelshohn, A., Monz, C., Dahmann, D., and Asbach, C.: Comparability of
877 mobility particle sizers and diffusion chargers, Journal of Aerosol Science, 57, 156-178,
878 http://dx.doi.org/10.1016/j.jaerosci.2012.10.008, 2013.

879 Kofahl, C.: Hochempfindliche Bestimmung der organischen und anorganischen Kohlenstoff-Fraktion in
880 Feinstaubproben mittels CRD-Spektroskopie, BS, Chemie und Biotechnologie, Fachhochschule Aachen, 2012.

881 Kuenen, J. J. P., Visschedijk, A. J. H., Jozwicka, M., and Denier van der Gon, H. A. C.: TNO-MACC_II
882 emission inventory; a multi-year (2003-2009) consistent high-resolution European emission inventory for air
883 quality modelling, Atmos. Chem. Phys., 14, 10963-10976, 10.5194/acp-14-10963-2014, 2014.

884 Lelieveld, J., Evans, J. S., Fnais, M., Giannadaki, D., and Pozzer, A.: The contribution of outdoor air pollution
885 sources to premature mortality on a global scale, Nature, 525, 367-371, 10.1038/nature15371, 2015.

886 Lindinger, W., Hirber, J., and Paretzke, H.: An ion/molecule-reaction mass spectrometer used for on-line trace
887 gas analysis, International Journal of Mass Spectrometry and Ion Processes, 129, 79-88,
888 http://dx.doi.org/10.1016/0168-1176(93)87031-M, 1993.

889 Liu, Y., Shao, M., Lu, S., Chang, C. C., Wang, J. L., and Chen, G.: Volatile Organic Compound (VOC)
890 measurements in the Pearl River Delta (PRD) region, China, Atmos. Chem. Phys., 8, 1531-1545, 10.5194/acp-8-
891 1531-2008, 2008.

892 Lough, G. C., Christensen, C. G., Schauer, J. J., Tortorelli, J., Mani, E., Lawson, D. R., Clark, N. N., and Gabele,
893 P. A.: Development of molecular marker source profiles for emissions from on-road gasoline and diesel vehicle
894 fleets, Journal of the Air & Waste Management Association (1995), 57, 1190-1199, 2007.

895 Mäki, M., Heinonsalo, J., Hellén, H., and Bäck, J.: Contribution of understorey vegetation and soil processes to
896 boreal forest isoprenoid exchange, Biogeosciences, 14, 1055-1073, 10.5194/bg-14-1055-2017, 2017.

897 Miyazaki, Y., Kawamura, K., Jung, J., Furutani, H., and Uematsu, M.: Latitudinal distributions of organic
898 nitrogen and organic carbon in marine aerosols over the western North Pacific, Atmos. Chem. Phys., 11, 3037-
899 3049, 10.5194/acp-11-3037-2011, 2011.

900 Mølgaard, B., Birmili, W., Clifford, S., Massling, A., Eleftheriadis, K., Norman, M., Vratolis, S., Wehner, B.,
901 Corander, J., Hämeri, K., and Hussein, T.: Evaluation of a statistical forecast model for size-fractioned urban
902 particle number concentrations using data from five European cities, Journal of Aerosol Science, 66, 96-110,
903 http://dx.doi.org/10.1016/j.jaerosci.2013.08.012, 2013.

904 Münkel, C.: Mixing height determination with lidar ceilometers results from Helsinki Testbed, Meteorologische
905 Zeitschrift, 16, 451-459, 10.1127/0941-2948/2007/0221, 2007.

906 Münkel, C., Schäfer, K., and Emeis, S.: Adding confidence levels and error bars to mixing layer heights detected
907 by ceilometer, 2011, 817708-817708-817709.

908 Park, S. S., Kim, Y. J., and Kang, C. H.: Atmospheric polycyclic aromatic hydrocarbons in Seoul, Korea, Atmos.
909 Environ., 36, 2917-2924, http://dx.doi.org/10.1016/S1352-2310(02)00206-6, 2002.

910 Putaud, J.-P., Raes, F., Van Dingenen, R., Brüggemann, E., Facchini, M. C., Decesari, S., Fuzzi, S., Gehrig, R.,
911 Hüglin, C., Laj, P., Lorbeer, G., Maenhaut, W., Mihalopoulos, N., Müller, K., Querol, X., Rodriguez, S.,
912 Schneider, J., Spindler, G., Brink, H. t., Tørseth, K., and Wiedensohler, A.: A European aerosol
913 phenomenology—2: chemical characteristics of particulate matter at kerbside, urban, rural and background sites
914 in Europe, Atmos. Environ., 38, 2579-2595, http://dx.doi.org/10.1016/j.atmosenv.2004.01.041, 2004.

915 Putaud, J. P., Van Dingenen, R., Alastuey, A., Bauer, H., Birmili, W., Cyrys, J., Flentje, H., Fuzzi, S., Gehrig,
916 R., Hansson, H. C., Harrison, R. M., Herrmann, H., Hitzenberger, R., Hüglin, C., Jones, A. M., Kasper-Giebl, A.,
917 Kiss, G., Kousa, A., Kuhlbusch, T. A. J., Löschau, G., Maenhaut, W., Molnar, A., Moreno, T., Pekkanen, J.,
918 Perrino, C., Pitz, M., Puxbaum, H., Querol, X., Rodriguez, S., Salma, I., Schwarz, J., Smolik, J., Schneider, J.,
919 Spindler, G., ten Brink, H., Tursic, J., Viana, M., Wiedensohler, A., and Raes, F.: A European aerosol
920 phenomenology – 3: Physical and chemical characteristics of particulate matter from 60 rural, urban, and
921 kerbside sites across Europe, Atmos. Environ., 44, 1308-1320,
922 http://dx.doi.org/10.1016/j.atmosenv.2009.12.011, 2010.

923 Rasmussen, D. J., Hu, J. L., Mahmud, A., and Kleeman, M. J.: The Ozone-Climate Penalty: Past, Present, and
924 Future, Environmental Science & Technology, 47, 14258-14266, 10.1021/es403446m, 2013.

925 Ravindra, K., Bencs, L., Wauters, E., de Hoog, J., Deutsch, F., Roekens, E., Bleux, N., Berghmans, P., and Van
926 Grieken, R.: Seasonal and site-specific variation in vapour and aerosol phase PAHs over Flanders (Belgium) and
927 their relation with anthropogenic activities, Atmos. Environ., 40, 771-785,
928 http://dx.doi.org/10.1016/j.atmosenv.2005.10.011, 2006.

929 Ravindra, K., Sokhi, R., and Van Grieken, R.: Atmospheric polycyclic aromatic hydrocarbons: Source
930 attribution, emission factors and regulation, Atmos. Environ., 42, 2895-2921,
931 http://dx.doi.org/10.1016/j.atmosenv.2007.12.010, 2008.

932 Rogge, W. F., Hildemann, L. M., Mazurek, M. A., Cass, G. R., and Simoneit, B. R. T.: Sources of fine organic
933 aerosol. 4. Particulate abrasion products from leaf surfaces of urban plants, Environmental Science &
934 Technology, 27, 2700-2711, 10.1021/es00049a008, 1993.

935 Rushdi, A. I., Al-Zarban, S., and Simoneit, B. R.: Chemical compositions and sources of organic matter in fine
936 particles of soils and sands from the vicinity of Kuwait city, Environ Monit Assess, 120, 537-557,
937 10.1007/s10661-005-9102-8, 2006.

938 Sannigrahi, P., Sullivan, A. P., Weber, R. J., and Ingall, E. D.: Characterization of Water-Soluble Organic
939 Carbon in Urban Atmospheric Aerosols Using Solid-State 13C NMR Spectroscopy, Environmental Science &
940 Technology, 40, 666-672, 10.1021/es051150i, 2006.

941 Schäfer, K., Blumenstock, T., Bonn, B., Gerwig, H., Hase, F., Münkel, C., Nothard, R., and Schneidemesser, E.
942 v.: Mixing layer height measurements determines influence of meteorology on air pollutant concentrations in
943 urban area, in: Remote Sensing of Clouds and the Atmosphere XX, edited by: Comerón, A., Kassianov, E. I.,
944 and Schäfer, K., Proceedings of SPIE, Bellingham, WA, USA, 2015.

945 Schäfer, K., Elsasser, M., Arteaga-Salas, J. M., Gu, J. W., Pitz, M., Schnelle-Kreis, J., Cyrys, J., Emeis, S.,
946 Prévôt, A. S. H., and Zimmermann, R.: Impact of meteorological conditions on airborne fine particle
947 composition and secondary pollutant characteristics in urban area during winter-time, Meteorologische
948 Zeitschrift, 25, 267-279, 2016.

949 Schauer, J. J., Rogge, W. F., Hildemann, L. M., Mazurek, M. A., Cass, G. R., and Simoneit, B. R. T.: Source
950 apportionment of airborne particulate matter using organic compounds as tracers, Atmos. Environ., 30, 3837-
951 3855, http://dx.doi.org/10.1016/1352-2310(96)00085-4, 1996.

952 Senatsverwaltung für Stadtentwicklung III F, B.: Informationssystem Stadt und Umwelt, Flächennutzung und
953 Stadtstruktur, Dokumentation der Kartiereinheiten und Aktualisierung des Datenbestandes, Berlin
954 Senatsverwaltung für Stadtentwicklung, Berlin, 2010.

955 Shen, R., Schäfer, K., Schnelle-Kreis, J., Shao, L., Norra, S., Kramar, U., Michalke, B., Abbaszade, G., Streibel,
956 T., Fricker, M., Chen, Y., Zimmermann, R., Emeis, S., and Schmid, H. P.: Characteristics and sources of PM in
957 seasonal perspective – A case study from one year continuously sampling in Beijing, Atmospheric Pollution
958 Research, 7, 235-248, http://dx.doi.org/10.1016/j.apr.2015.09.008, 2016.

959 Simoneit, B. R. T.: Organic matter of the troposphere—III. Characterization and sources of petroleum and
960 pyrogenic residues in aerosols over the western united states, Atmospheric Environment (1967), 18, 51-67,
961 http://dx.doi.org/10.1016/0004-6981(84)90228-2, 1984.

962 Simoneit, B. R. T.: Characterization of Organic Constituents in Aerosols in Relation to Their rigin and
963 Transport: A Review, International Journal of Environmental Analytical Chemistry, 23, 207-237,
964 10.1080/03067318608076446, 1986.

965 Simoneit, B. R. T., Schauer, J. J., Nolte, C. G., Oros, D. R., Elias, V. O., Fraser, M. P., Rogge, W. F., and Cass,
966 G. R.: Levoglucosan, a tracer for cellulose in biomass burning and atmospheric particles, Atmos. Environ., 33,
967 173-182, http://dx.doi.org/10.1016/S1352-2310(98)00145-9, 1999.

968 Simoneit, B. R. T.: Biomass burning — a review of organic tracers for smoke from incomplete combustion,
969 Applied Geochemistry, 17, 129-162, http://dx.doi.org/10.1016/S0883-2927(01)00061-0, 2002.

970 Stein, A. F., Draxler, R. R., Rolph, G. D., Stunder, B. J. B., Cohen, M. D., and Ngan, F.: NOAA's HYSPLIT
971 Atmospheric Transport and Dispersion Modeling System, Bulletin of the American Meteorological Society, 96,
972 2059-2077, 10.1175/bams-d-14-00110.1, 2015.

973 Stülpnagel, A. v., Kaupp, H., Nothard, R., Preuß, J., Preuß, M., Clemen, S., and Grunow, K.: Luftgütemessdaten
974 2014, Senatsverwaltung für Stadtentwicklung und Umwelt, Berlin, 2015.

975 Tang, G., Zhang, J., Zhu, X., Song, T., Münkel, C., Hu, B., Schäfer, K., Liu, Z., Zhang, J., Wang, L., Xin, J.,
976 Suppan, P., and Wang, Y.: Mixing layer height and its implications for air pollution over Beijing, China, Atmos.
977 Chem. Phys., 16, 2459-2475, 10.5194/acp-16-2459-2016, 2016.

978 Thijsse, T. R., van Oss, R. F., and Lenschow, P.: Determination of Source Contributions to Ambient Volatile
979 Organic Compound Concentrations in Berlin, Journal of the Air & Waste Management Association, 49, 1394-
980 1404, 10.1080/10473289.1999.10463974, 1999.

981 Urban, S.: Charakterisierung der Quellverteilung von Feinstaub und Stickoxiden in ländlichem und städtischem
982 Gebiet, PhD, Mathematik und Naturwissenschaften, Bergischen Universität Wuppertal, Wuppertal, Germany,
983 2010.

984 VDI: VDI Richlinie 3871: Messen von Partikeln in der Außenluft - Elektrische Aerosolmonitore auf Basis der
985 Diffusionsaufladung, in, edited by: Ingenieure, V. D., 2017.

986 Villalobos, A. M., Barraza, F., Jorquera, H., and Schauer, J. J.: Chemical speciation and source apportionment of
987 fine particulate matter in Santiago, Chile, 2013, Science of The Total Environment, 512–513, 133-142,
988 http://dx.doi.org/10.1016/j.scitotenv.2015.01.006, 2015.

989 Volz-Thomas, A., Geiss, H., Hofzumahaus, A., and Becker, K. H.: Introduction to special section:
990 Photochemistry experiment in BERLIOZ, Journal of Geophysical Research D: Atmospheres, 108, 1-1, 2003.

991 von Schneidemesser, E., Monks, P. S., Gros, V., Gauduin, J., and Sanchez, O.: How important is biogenic
992 isoprene in an urban environment? A study in London and Paris, Geophysical Research Letters, 38,
993 10.1029/2011GL048647, 2011.

994 Wang, Y., Zhuang, G., Tang, A., Yuan, H., Sun, Y., Chen, S., and Zheng, A.: The ion chemistry and the source
995 of PM2.5 aerosol in Beijing, Atmos. Environ., 39, 3771-3784, http://dx.doi.org/10.1016/j.atmosenv.2005.03.013,
996 2005.

997 Watson, J. G., Cooper, J. A., and Huntzicker, J. J.: The effective variance weighting for least squares
998 calculations applied to the mass balance receptor model, Atmospheric Environment (1967), 18, 1347-1355,
999 http://dx.doi.org/10.1016/0004-6981(84)90043-X, 1984.

1000 Weinhold, K.: personal communication, in, edited by: Gerwig, H., 2014.

1001 West, J. J., Smith, S. J., Silva, R. A., Naik, V., Zhang, Y., Adelman, Z., Fry, M. M., Anenberg, S., Horowitz, L.
1002 W., and Lamarque, J.-F.: Co-benefits of mitigating global greenhouse gas emissions for future air quality and
1003 human health, Nature Clim. Change, 3, 885-889, 10.1038/nclimate2009

1004 http://www.nature.com/nclimate/journal/v3/n10/abs/nclimate2009.html#supplementary-information, 2013.

1005 Whalley, L. K., Stone, D., Bandy, B., Dunmore, R., Hamilton, J. F., Hopkins, J., Lee, J. D., Lewis, A. C., and
1006 Heard, D. E.: Atmospheric OH reactivity in central London: observations, model predictions and estimates of in
1007 situ ozone production, Atmos. Chem. Phys., 16, 2109-2122, 10.5194/acp-16-2109-2016, 2016.

1008 WHO: WHO releases country estimates on air pollution exposure and health impact, in, World Health
1009 Organization, Geneva, 2016.

1010 Wiedensohler, A., Wiesner, A., Weinhold, K., Birmili, W., Hermann, M., Merkel, M., Müller, T., Pfeifer, S.,
1011 Schmidt, A., Tuch, T., Velarde, F., Quincey, P., Seeger, S., and Nowak, A.: Mobility Particle Size
1012 Spectrometers: Calibration Procedures and Measurement Uncertainties, Aerosol Science and Technology,
1013 10.1080/02786826.2017.1387229, 2017.

1014 Wiegner, M., Madonna, F., Binietoglou, I., Forkel, R., Gasteiger, J., Geiß, A., Pappalardo, G., Schäfer, K., and
1015 Thomas, W.: What is the benefit of ceilometers for aerosol remote sensing? An answer from EARLINET,
1016 Atmospheric Measurement Techniques, 7, 1979-1997, 10.5194/amt-7-1979-2014, 2014.

1017 Wiegner, M., and Gasteiger, J.: Correction of water vapor absorption for aerosol remote sensing with
1018 ceilometers, Atmos. Meas. Tech., 8, 3971-3984, 10.5194/amt-8-3971-2015, 2015.

1019 Winkler, J., Blank, P., Glaser, K., Gomes, J. A. G., Habram, M., Jambert, C., Jaeschke, W., Konrad, S.,
1020 Kurtenbach, R., Lenschow, P., Lörzer, J. C., Perros, P. E., Pesch, M., Prümke, H. J., Rappenglück, B., Schmitz,
1021 T., Slemr, F., Volz-Thomas, A., and Wickert, B.: Ground-Based and Airborne Measurements of Nonmethane
1022 Hydrocarbons in BERLIOZ: Analysis and Selected Results, Journal of Atmospheric Chemistry, 42, 465-492,
1023 10.1023/a:1015709214016, 2002.

1024 WorldBank: The Cost of Air Pollution : Strengthening the Economic Case for Action, World Bank, Washington,
1025 DC, 2016.

1026 Yang, H., Li, Q., and Yu, J. Z.: Comparison of two methods for the determination of water-soluble organic
1027 carbon in atmospheric particles, Atmos. Environ., 37, 865-870, http://dx.doi.org/10.1016/S1352-2310(02)00953-
1028 6, 2003.

1029 Zhang, T., Claeys, M., Cachier, H., Dong, S., Wang, W., Maenhaut, W., and Liu, X.: Identification and
1030 estimation of the biomass burning contribution to Beijing aerosol using levoglucosan as a molecular marker,
1031 Atmos. Environ., 42, 7013-7021, http://dx.doi.org/10.1016/j.atmosenv.2008.04.050, 2008.

1032

1033
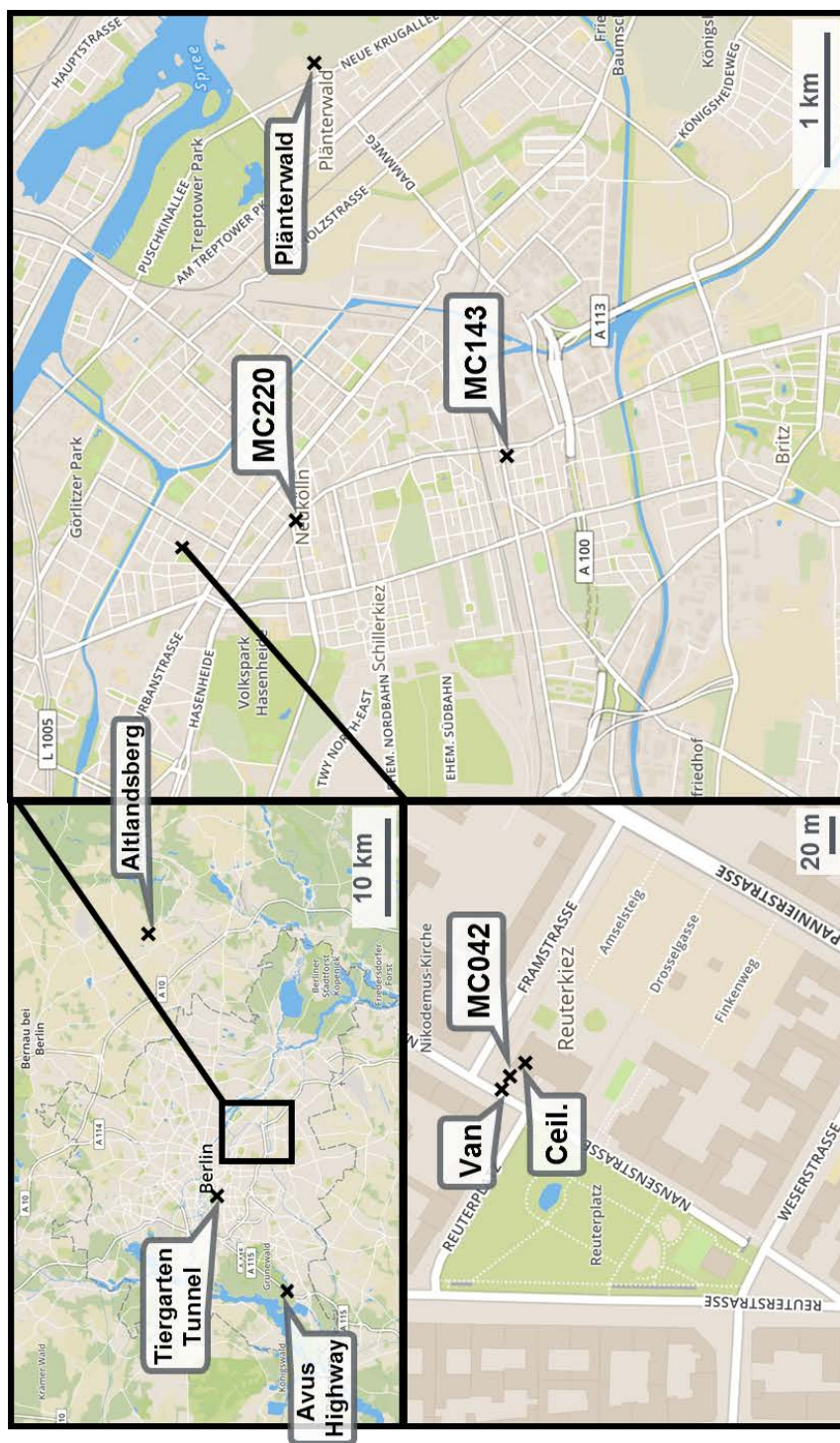
Figure 1. Location of the measurement station (MC042) and measurement van in Neukölln, Berlin. Maps show increasingly larger scale. The 'x's indicate sampling locations, with MC220 and MC143 indicating stations that record traffic counts. Map images from OpenStreetMap.
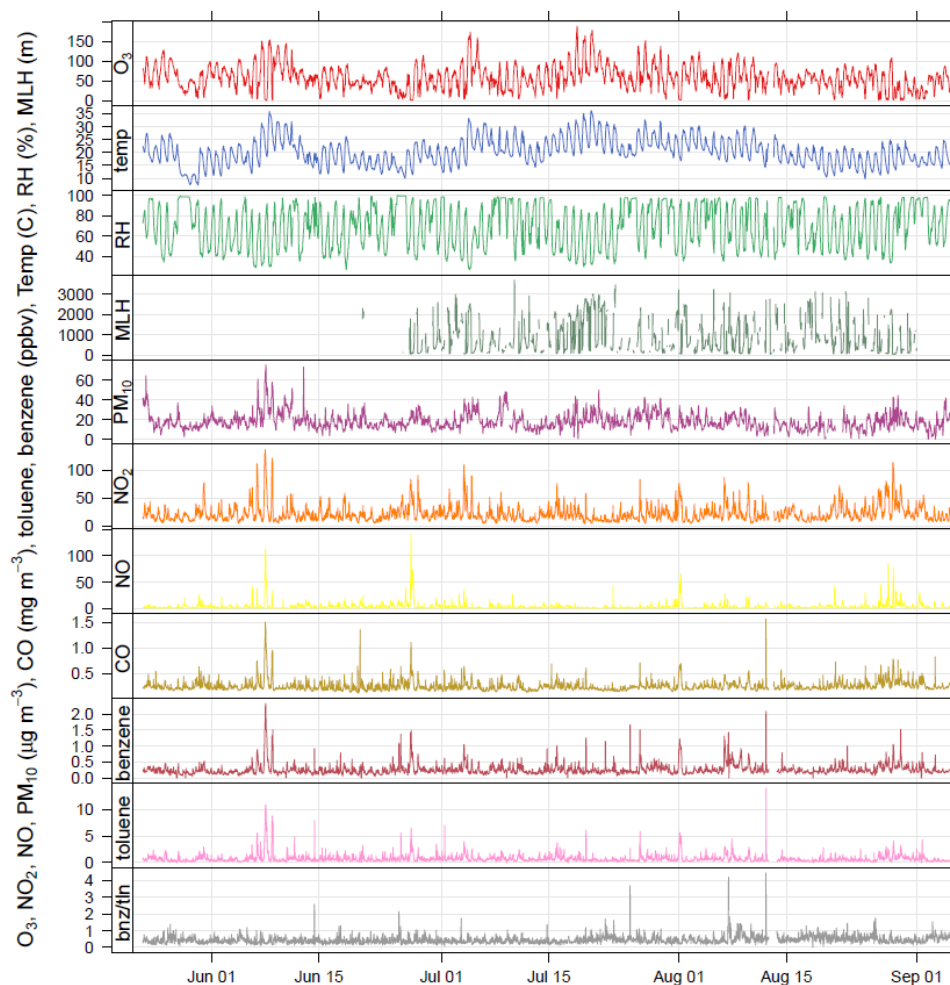
Figure 2. Time series of air pollutant concentrations, meteorological data, and benzene/toluene ratio measured as part of BLUME at the Neukölln station during the BAERLIN2014 campaign.
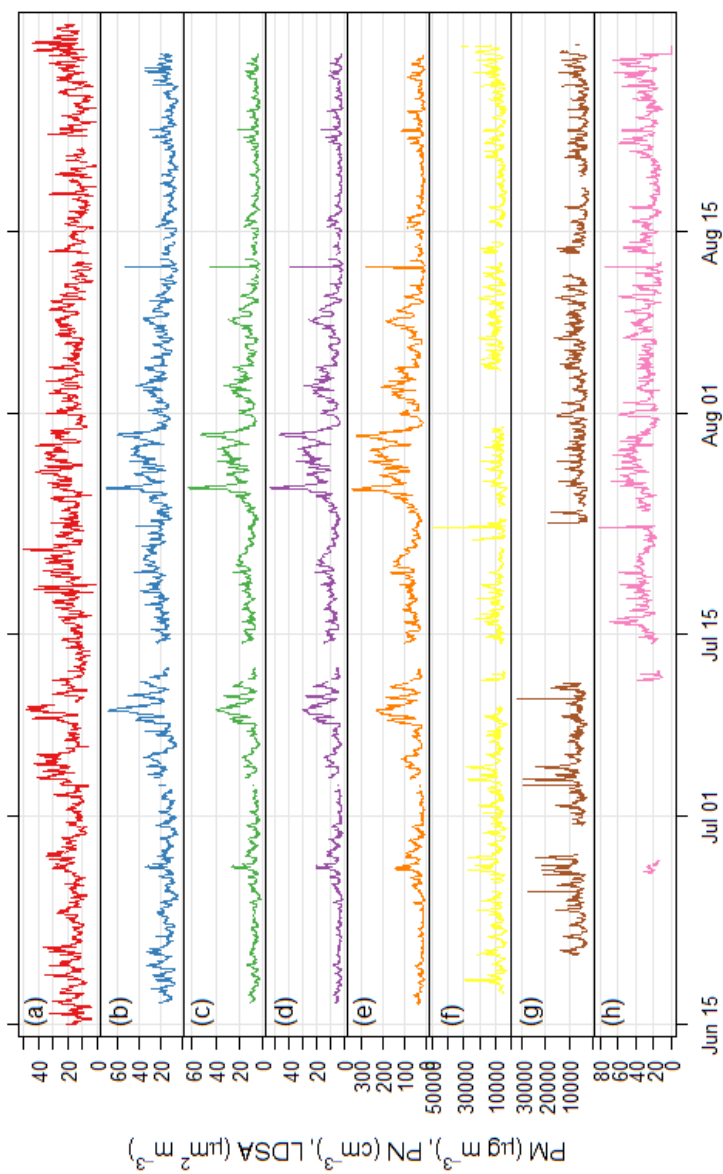
Figure 3. Time series of particulate matter mass, particle number, and lung depositable surface area concentrations measured at the Neukölln station during the BAERLIN2014 campaign. (a) BLUME PM10, (b) Grimm 1.108 PM10, (c) Grimm 1.108 PM2.5, (d) Grimm 1.108 PM1, (e) Grimm 1.108 PN, (f) Grimm 5.416 PN, (g) Grimm 5.403 PN, (h) NSAM LDSA. Units given in the y-axis label.
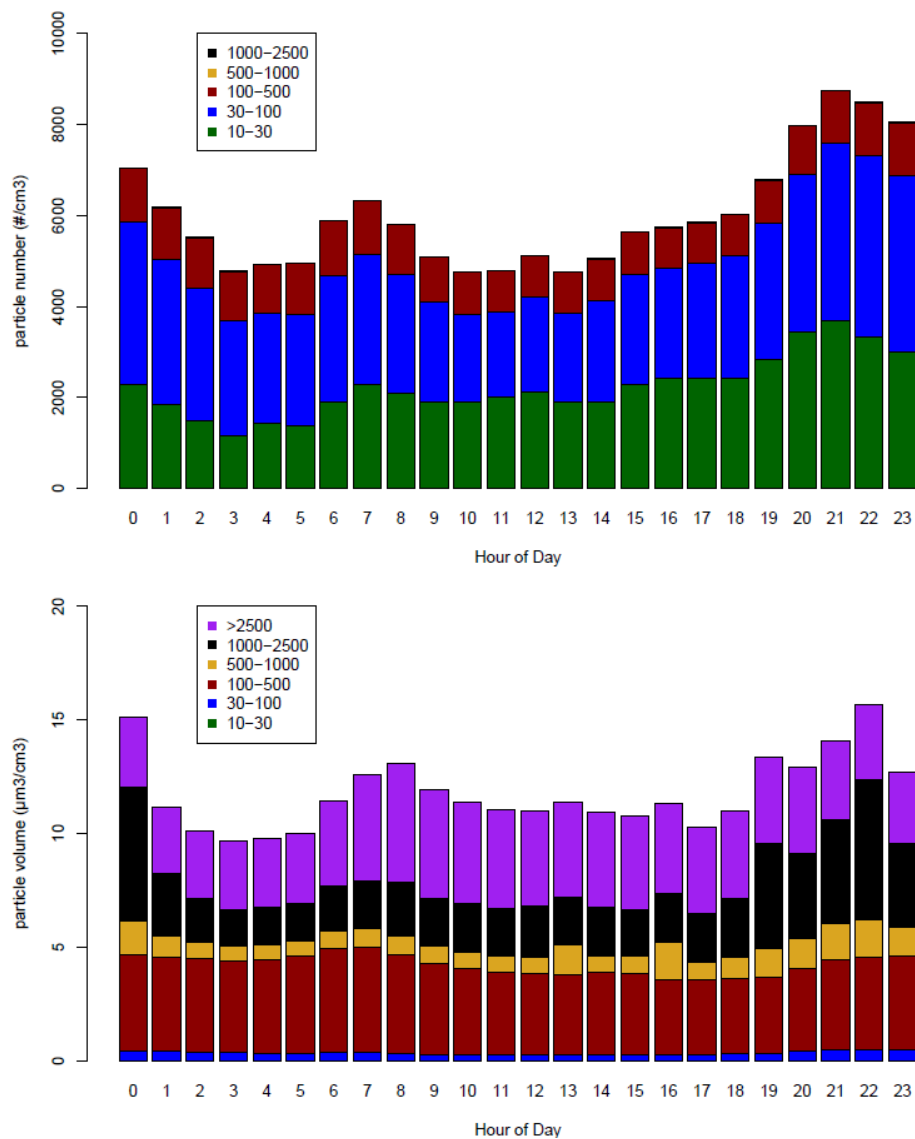
Figure 4. Mean diurnal cycles of the (top) particle number and (bottom) particle volume distributions at Neukölln. Legends show particle size bin range in nm.
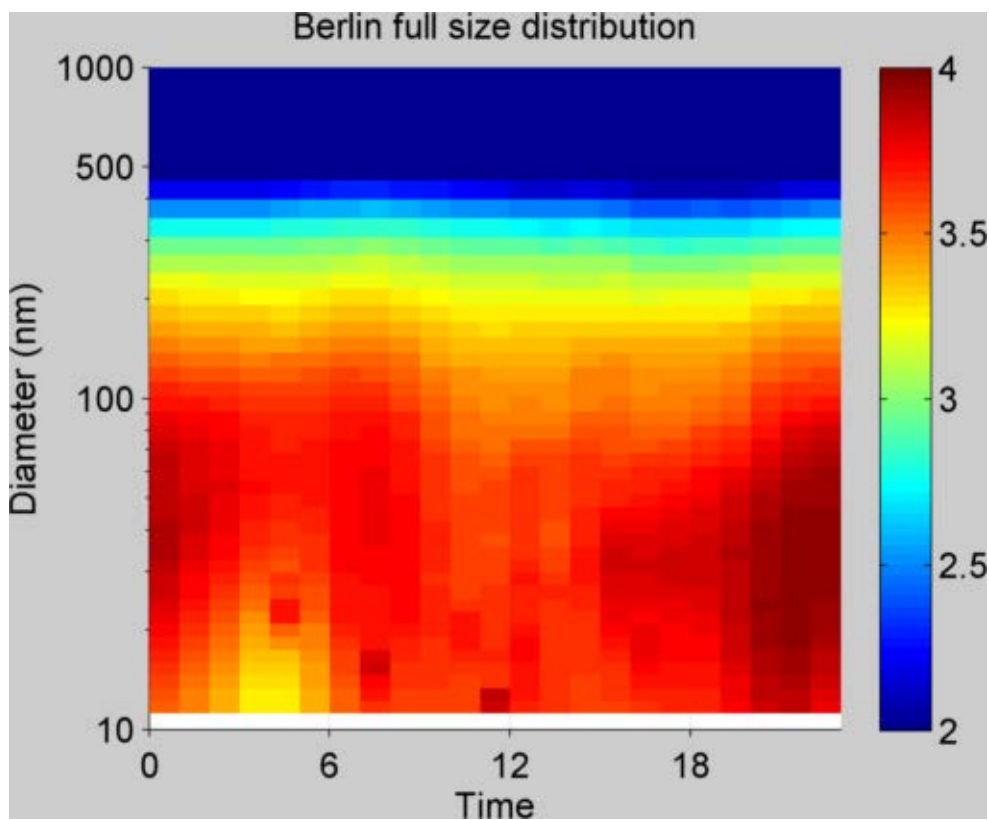
Figure 5. Mean diurnal cycle of the particle number concentration by diameter.
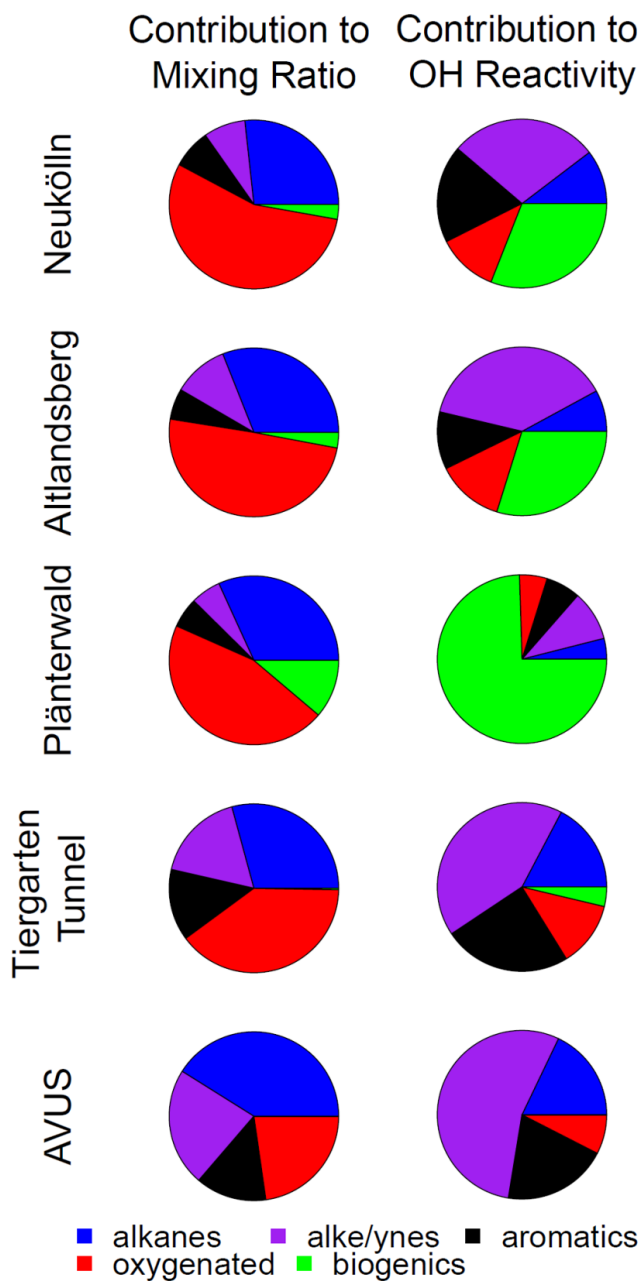
Figure 6. Mean fractional contribution to mixing ratio (left column) and OH reactivity (right column) by compound class, based on a total mixing ratio or OH reactivity calculated from 57 compounds for 5 sampling locations throughout the city. Total number of canister samples for each location are Neukölln (18), Altlandsberg (10), Plänterwald (11), Tiergarten Tunnel (9), and the AVUS (2). The individual compounds included in each class are available in the SI.
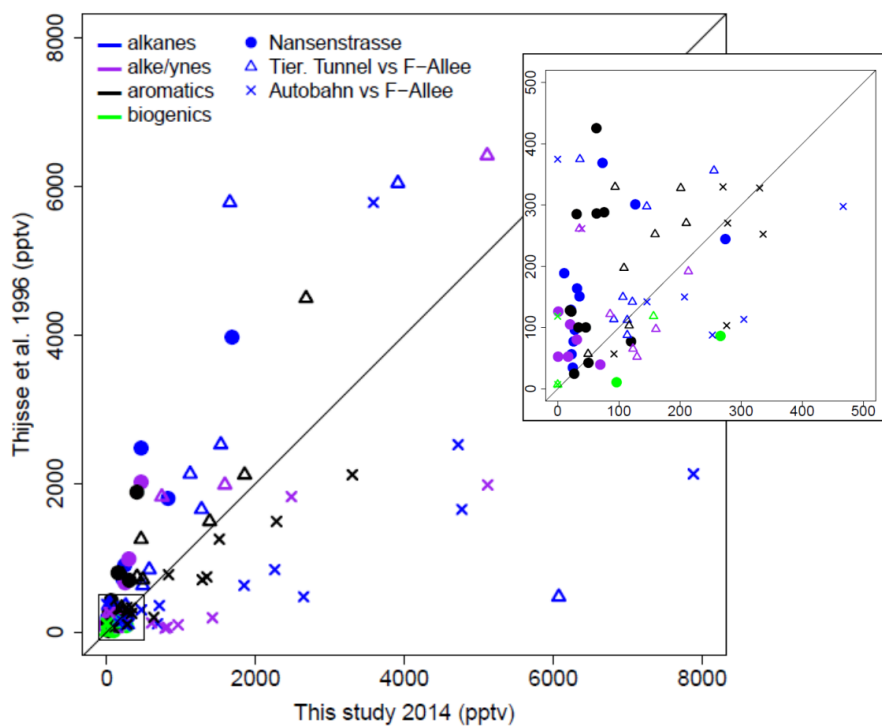
Figure 7. Comparison between VOC measurements in this study and comparable previous work from June-August of 1996 (Thijsse et al., 1999). Compound classes are distinguished by color. Sampling locations by character.
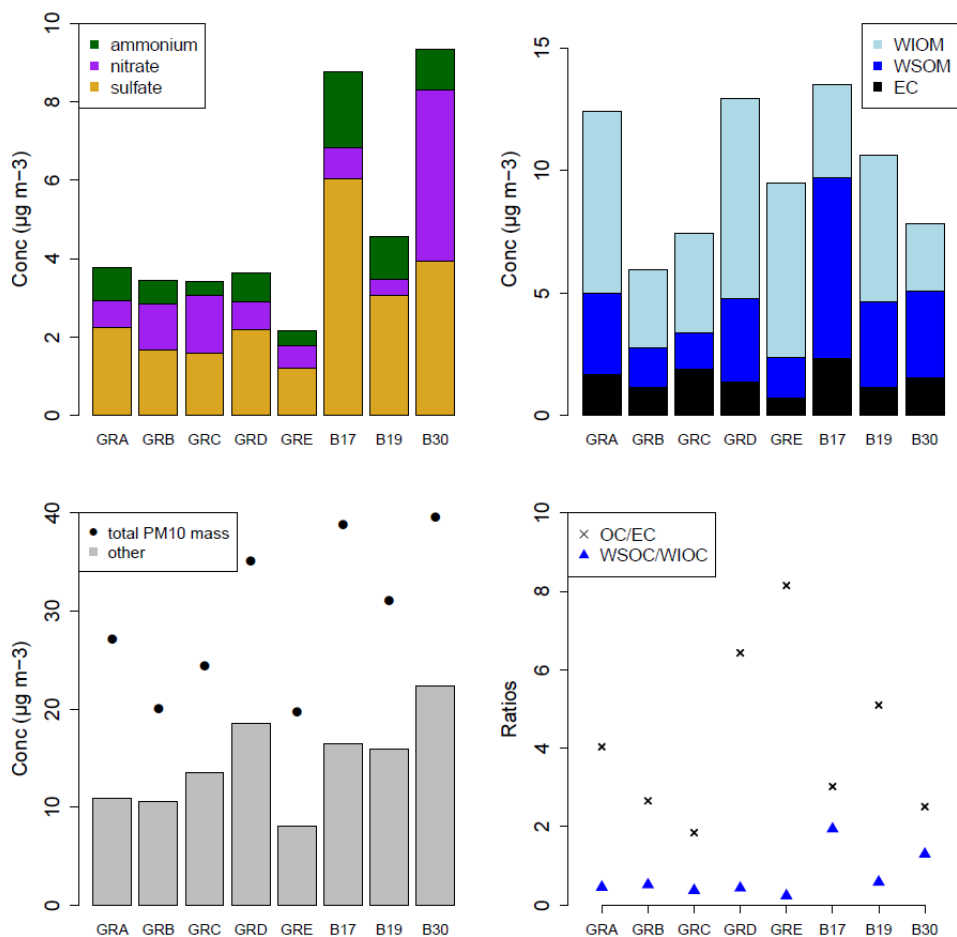
Figure 8. Bulk composition analysis results from the PM10 filter samples, presented by filter groups, where GRA=Group A, GRB=Group B, etc. and B17, B19, B30 are individual filters. More information on the filter groups, including a some basic composition information and backtrajectory origin can be found in Table 3.
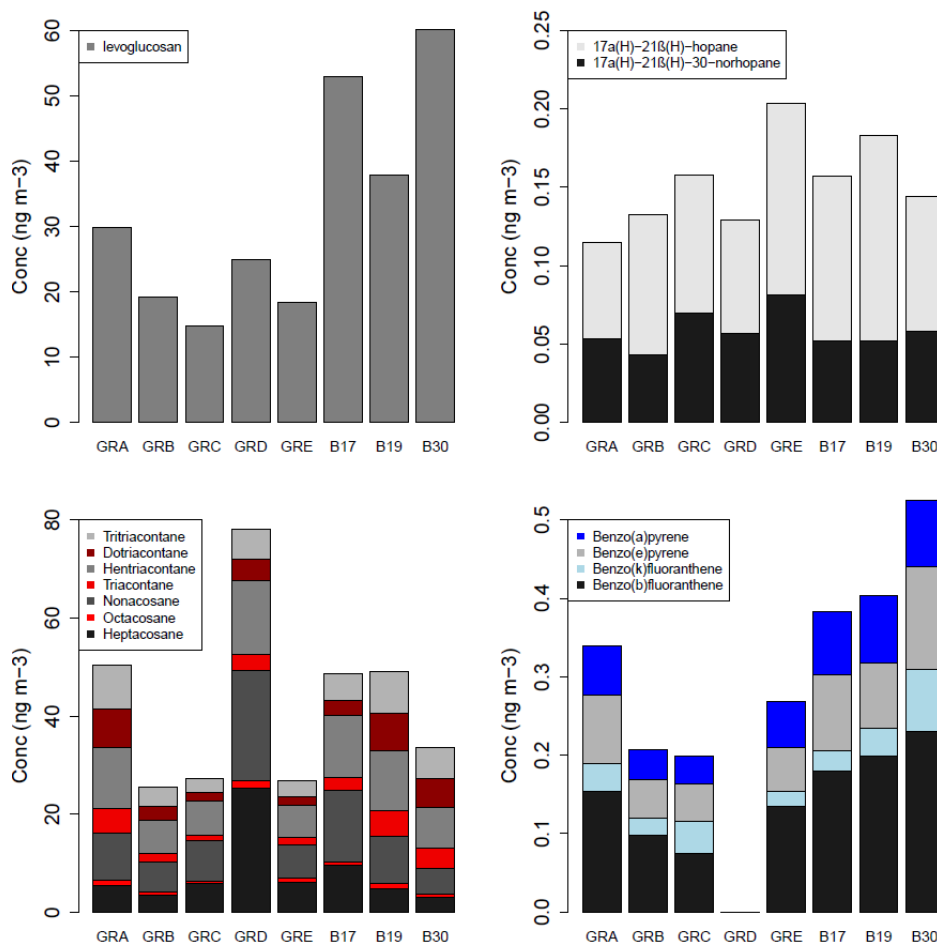
Figure 9. Molecular marker analysis results from the PM10 filter samples, presented by filter groups, where GRA=Group A, GRB=Group B, etc. and B17, B19, B30 are individual filters. More information on the filter groups, including a some basic composition information and backtrajectory origin can be found in Table 3.
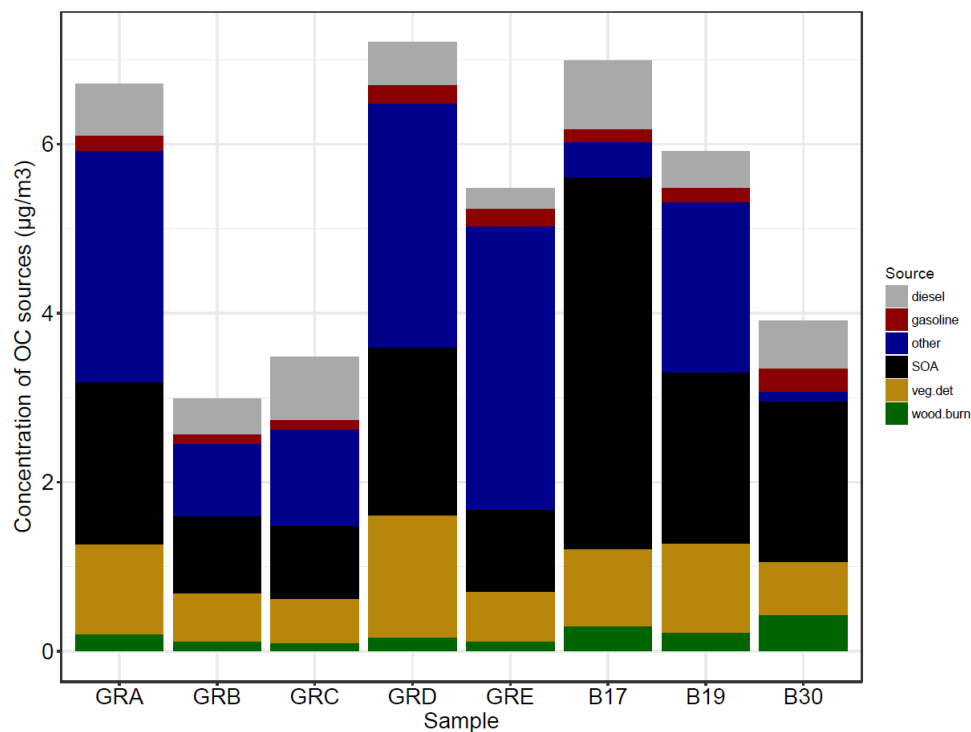
Figure 10. Source contributions attributed to the OC fraction of the PM10 filter samples by filter groups, where GRA=Group A, GRB=Group B, etc. and B17, B19, B30 are individual filters. More information on the filter groups, including a some basic composition information and backtrajectory origin can be found in Table 3.

Table 1. List of participating institutions and instruments deployed at the urban background site in Berlin (Nansenstrasse).

Institution	Instrument	Parameters	References
Berlin Senate	Leckel GmbH SEQ47/50 (x1)	PM_{10}	DIN EN 16450:2015-10: Beuth, 2015
	Horiba APNA-370 Air Pollution Monitor	NOx, NO (measured directly); NO_2 (inferred)	DIN EN 14211:2005; Verbraucherschutz, 2010
	Horiba APOA-370 Air Pollution Monitor	O_3	DIN EN 14625:2005; Verbraucherschutz, 2010
	Horiba APMA-370 Air Pollution Monitor	CO	DIN EN 14626:2005; Verbraucherschutz, 2010
	AMA Instruments GC5000 BTX	Benzene, toluene	DIN EN 14662:2005; Verbraucherschutz, 2010
KIT	Vaisala CL51 Ceilometer	Mixing layer height	Emeis et al., 2007; Münkel et al., 2007; Wiegner et al., 2014
UBA	GRIMM 1.108	Particle number and size distribution (350-22500 nm), 15 size bins	Görner et al. 2012
	GRIMM 5.403	Particle number and size distribution (10-1100 nm), 44 size bins	Heim et al., 2004
	GRIMM 5.416	Total particle number (4-3000 nm)	Helsper et al., 2008; Wiedensohler et al., 2017
	NSAM	Particle surface area (10-1000 nm)	Kaminski et al., 2013; VDI 2017
IASS	PTR-MS	NMVOCs (for a complete list of m/z see Table S1)	Bourtsoukidis et al. 2014
FZJ	Canister samples	NMVOCs (for a list of compounds, see Table 8 in Bonn et al., 2016, or for the 57 compounds included in this analysis the SI)	Urban 2010; Ehlers et al. 2016
	Filter sampling/analysis	PM_{10} mass, EC, OC	Kofahl 2012; Ehlers 2013
FMI-Helsinki	Cartridge samples	Biogenic NMVOCs	Mäki et al. 2017
UW-Madison	Filter analysis	WSOC, WIOC, ions, organic tracers	Yang et al., 2003; Wang et al., 2005; Miyazaki et al., 2011; Villalobos et al., 2015

Table 2. NMVOC canister sampling locations, site type, and average OH reactivity (s^{-1})

	Location type	alkanes	alkenes	aromatics	oxygenated	biogenics	total
Neukölln†	Urban background station	0.27±0.10	0.75±0.40	0.49±0.29	0.29±0.08	0.82±0.44	2.6±0.68
Altlandsberg	Rural, agricultural area with a small town, partially forested	0.17±0.10	0.83±0.43	0.22±0.11	0.28±0.17	0.65±0.42	2.2±0.69
Plänterwald	ca. 1 km² urban park abutting the Spree river in eastern Berlin	0.20±0.06	0.47±0.14	0.33±0.12	0.25±0.04	3.7±0.90	4.9±1.0
Tiergarten Tunnel*	2.4 km tunnel, major 4-lane city thoroughfare in central Berlin	2.0±2.2	4.4±1.1	2.6±1.3	1.3±0.70	0.39±0.24	11±2.5
AVUS*	Highly traficked motorway in western Berlin (traffic jam)	6.3±3.2	19±7.4	6.6±1.6	2.8±2.3	0.00±0.00	34±15

* automated sampling while driving; all other samples taken from a stationary location.
† 20 minute sampling duration. All other samples had 10 minute sampling duration.

Table 3. Basic bulk composition results, ratios, and air mass origin from HYSPLIT. Units are µg m-3 unless otherwise noted. For OC and ED measurement uncertainty is included.

	Total PM10	Air mass origin (HYSPLIT)	Total OC (± unc)	Total EC (± unc)	Total Ions*	OC:EC ratio	WSOC of OC (%)	Ions:OC ratio**
Group A	27.1	Germany	6.7 ± 0.34	1.7 ± 0.084	5.1	4.0	31%	0.56
Group B	20.0	central Germany, northern France	3.0 ± 0.15	1.1 ± 0.057	5.3	2.7	34%	1.2
Group C	24.4	North Sea	3.5 ± 0.17	1.9 ± 0.094	5.7	1.8	27%	0.98
Group D	35.1	Baltic	7.2 ± 0.36	1.4 ± 0.069	5.0	6.4	30%	0.50
Group E	19.6	North Sea, Scandinavia, UK	5.5 ± 0.27	0.71 ± 0.035	3.2	8.1	19%	0.39
B17	38.8	Poland & east	7.0 ± 0.35	2.3 ± 0.12	11	3.0	66%	1.3
B19	31.0	Poland & north	5.9 ± 0.30	1.2 ± 0.058	6.0	5.1	37%	0.77
B30	39.5	Germany (northern France)	3.9 ± 0.20	1.6 ± 0.078	15	2.5	56%	2.4

*Ions includes 7 species and is not limited to sulfate, nitrate, and ammonium.
**Ratio of ions (sulfate, nitrate, ammonium) to OC

Table 4. Chemical mass balance source apportionment results. Units are µg m-3 unless otherwise noted. Uncertainty is measurement uncertainty, in the case of SOA propagated uncertainty.

	Total OC (unc)	% OC mass apportioned	measured WSOC (unc)	SOA* (unc)	veg. det. (std error)	wood burn. (std error)	diesel emissions (std error)	gasoline vehicles (std error)	R^2	χ^2
Group A	6.71±0.34	30.8	2.06±0.10	1.91±0.11	1.07±0.13	0.21±0.04	0.61±0.06	0.19±0.02	0.77	12.39
Group B	2.99±0.15	41.2	1.00±0.05	0.91±0.05	0.57±0.07	0.12±0.03	0.42±0.04	0.12±0.02	0.8	7.7
Group C	3.48±0.17	42.4	0.94±0.05	0.87±0.05	0.52±0.06	0.10±0.02	0.74±0.07	0.11±0.02	0.85	5.38
Group D	7.21±0.36	32.3	2.11±0.11	1.99±0.11	1.44±0.17	0.17±0.04	0.50±0.05	0.22±0.03	0.87	6.82
Group E	5.48±0.27	21.2	1.05±0.05	0.97±0.06	0.59±0.07	0.12±0.03	0.24±0.03	0.21±0.02	0.77	9.78
B17	6.99±0.35	31.1	4.61±0.23	4.40±0.24	0.91±0.10	0.30±0.07	0.81±0.08	0.15±0.03	0.8	7.89
B19	5.91±0.30	31.7	2.19±0.11	2.03±0.12	1.05±0.12	0.22±0.05	0.42±0.04	0.18±0.03	0.73	9.83
B30	3.91±0.20	48.6	2.21±0.11	1.90±0.13	0.63±0.08	0.44±0.09	0.57±0.06	0.28±0.04	0.76	10.17

*The SOA contribution was not part of the CMB results, but rather calculated as: unapportioned WSOC (SOA) = measured WSOC – 0.71*apportioned wood burning.